COMPUTATIONAL FLUID DYNAMICS ANALYSIS & MODIFICATION OF SOLAR PHOTOVOLTAIC (PV) MODULES

Submitted by:

Muhammad Khalilullah Tunio

Supervised by:

Dr. Shafique ur Rehman

THESIS

Submitted to:

Department of Mechanical Engineering

Pakistan Navy Engineering College Karachi

National University of Science and Technology, Islamabad Pakistan

In partial fulfillment of requirement for the award of the degree of

MASTER OF SCIENCE IN MECHANICAL ENGINEERING

With Specialization in Thermal Power

August 2015

ACKNOWLEDGEMENT

I am very fortunate to be involved in this research project. This study increases my knowledge to understand the CFD and solar power technology. Professionally as solar power specialist, this study increase my thinking, knowledge and understandings capability to manage the solar power technology successfully.

I would like to sincerely thank my supervisor Dr. Shafique ur Rehman for his excellent guidance and support throughout this study. I would also express my gratitude to Dr. M.Nouman Qureshi (SUPARCO) and Dr Nasim A. Khan (Ex. VC Hamdard University) whose motivation and guidance help me to understand the CFD and solar power technology. Finally, I would like to acknowledge with gratitude, the support and love of my Parents.

Proposed Certificate for Plagiarism

1. It is certified that MS Thesis Titled "Computational Fluid Dynamics Analysis and Modification of Solar Photovoltaic Modules" by Muhammad Khalilullah (2011-NUST-MS-Phd Mech (N) 09) has been examined by us. We undertake the follows:

   a. The work presented is original and own work of the author (i.e. there is no plagiarism). No ideas, processes, results, or words of others have been presented as an Author own work.

   b. Thesis has significant new work / knowledge as compared already published or are under consideration to be published elsewhere. No sentence, equation, diagram, table, paragraph or section has been copied verbatim from previous work unless it is placed under quotation marks and duly referenced.

   c. There is no falsification by manipulating research materials, equipment, or processes, or changing or omitting data or results such that the research is not accurately represented in the research record.

   d. The thesis has been checked using TURNITIN (copy of originality report attached) and found within limits as per HEC Plagiarism Policy and instructions issued from time to time.

Name & Signature of Supervisor

ABSTRACT

Solar photovoltaic (PV) is one of the growing renewable energy technologies and playing a key role in supplying electricity for many applications. Though it is considered as a fuel-free energy source, yet its utilization is limited due to lower conversion efficiencies and higher cost. With the help of latest engineering technologies, only 16% of energy captured from the sun can be converted into the electricity by using solar PV modules/panels. One of the basic problems in PV technology is that, the efficiency of PV panels decrease with the increase in operating temperature (at the base of cell). The maximum efficiency of PV cell have been designed at 25˚C and above 40˚C ambient temperature is normal in this region, therefore an increase in temperature that is proportional to the cell temperature would cause the voltage drops that is proportional in decrement of power and efficiency as discussed. One way to increase the efficiency and to reduce the cell temperature by attaching a duct with back plate of the cell. This generates airflow due to natural convection. Moving air therefore removes the heat generated in PV cell. This study reports the CFD analysis of the duct arrangements for cooling of the cell. Study determines the effect of temperature in the cell with air gap at the base. An Air Gap (Air flow) was introduced at the base of cell which dissipated heat away from the cell and thus enhanced the efficiency of panel by maintaining the temperature of the panel. The relation of cell temperature with power and efficiency of the cell have been studied in this study. The maximum temperature, power and efficiency difference between the normal and CFD modified PV cell were achieved upto 12˚C, 0.21W and 0.21%.

TABLE OF CONTENTS

LIST OF FIGURES

LIST OF GRAPH

NOMENCLATURE

Acronyms:

CFD	Computational Fluid Dynamics
PV	Photovoltaic Module
CPV	Concentrated Photovoltaic
DI	Densely Ionized
EVA	Ethyl Vinyl Acetate
TPT	Tedlar Pet Tedlar
PVF	Poly Vinyl Fluoride
Voc	Open Circuit Voltage
Isc	Short Circuit Current
Vmp	Voltage at maximum power
Imp	Current at maximum power
S	Solar Insolation
NOCT	Normal Operating Cell Temperature
STC	Standard Testing Condition
H_{trans}	Transmitted Heat Flux
H_{irrad}	Solar Irradiance
H_{rad}	Radiation Losses
H_r	Remaining Heat
T_{cell}	Cell Temperature

Greek symbols

η	Efficiency
Eg	Energy Bandgap
μ	Dynamic Viscosity
e	Emissivity of absorber plate
Re	Reynolds number
Nu	Nusselt number for roughened duct
k	Thermal conductivity of air (W/m/K)
L	Length of duct (m)
A	Area
$\tau\alpha$	Transmittance–absorptance
ρ	Density of air(kg/m^3)

1 INTRODUCTION

1.1 Introduction

In this thesis, project titled **"Computational Fluid Dynamics Analysis and Modification of Solar Photovoltaic Modules"** was carried out.

In 1st chapter, introduction of research work with scope of study and energy scenario of the country has been described in detail.

In 2nd chapter, literature review is characterized by a logical flow of ideas; current and relevant references with consistent, appropriate referencing style; proper use of terminology; and an unbiased and comprehensive view of the previous research on the temperature effects on photovoltaic modules.
In 3rd chapter, construction, working principle and behavior of solar PV technology has been described in detail.

In 4th chapter, an analysis of experimental patent work to be carried out for computational fluid dynamics is included.

In 5th chapter, the introduction of problem to be simulated in computational fluid dynamics through software and methodology of work has been described in detail with governing equations, assumptions and calculations.

In 6th chapter, CFD results and its comparison with experimental has been described in detail.

The 7th chapter describes the conclusion of the results and suggests further recommendations for future works.

1.2 Energy scenario in Pakistan

Energy is one of the main inputs for economic development of any country. For developing countries, the energy sector assumes a fundamental importance in view of the needs of increasing energy as a large investment is required to meet them.

Pakistan is facing a serious energy crisis in its history due to the increase in energy demand and lack of investment in the mobilization of its energy resources. The Pakistani government is committed to increasing the supply of energy for economic and social development in the country, in a sustainable manner. In order to reduce imported energy charge, the government is utilizing all its capabilities and resources to increase the native energy supply and is seeking private investment to increase exploration and production of hydrocarbons and the exploitation of domestic coal resources sector for power generation. With limited availability of fossil fuels, the utilization of renewable energy is another area where many countries are moving on fast track basis [1]

1.3 Renewable Energy Potential

The role of renewable energy is very important in the future, power that produce from renewable energy is competitively is more financially beneficial as compare to conventional sources.

Pakistan is blessed with various renewable energy resources such as hydel, solar, wind, geothermal and biofuels. From the latest statistics, Renewable energy potential in the country is as follows: [1]

Source	Capacity
Solar	2900000 MW
Wind	340000 MW
Hydro (large)	50000 MW
Hydro (small)	3100 MW
Baggase cogeneration	1800 MW
Waste to power	500 MW
Geothermal	500 MW

1.4 Solar Energy

Solar energy is radiant energy and is produced in the sun as a result of nuclear fusion reactions. It is transmitted to the earth in shape of energy called photons. Solar energy is considered as the

most suitable energy available all over the world that can play a vital role to reduce energy gap and transmission losses by providing electricity in remote areas. Photovoltaic (PV) cells convert sunlight directly into electricity.

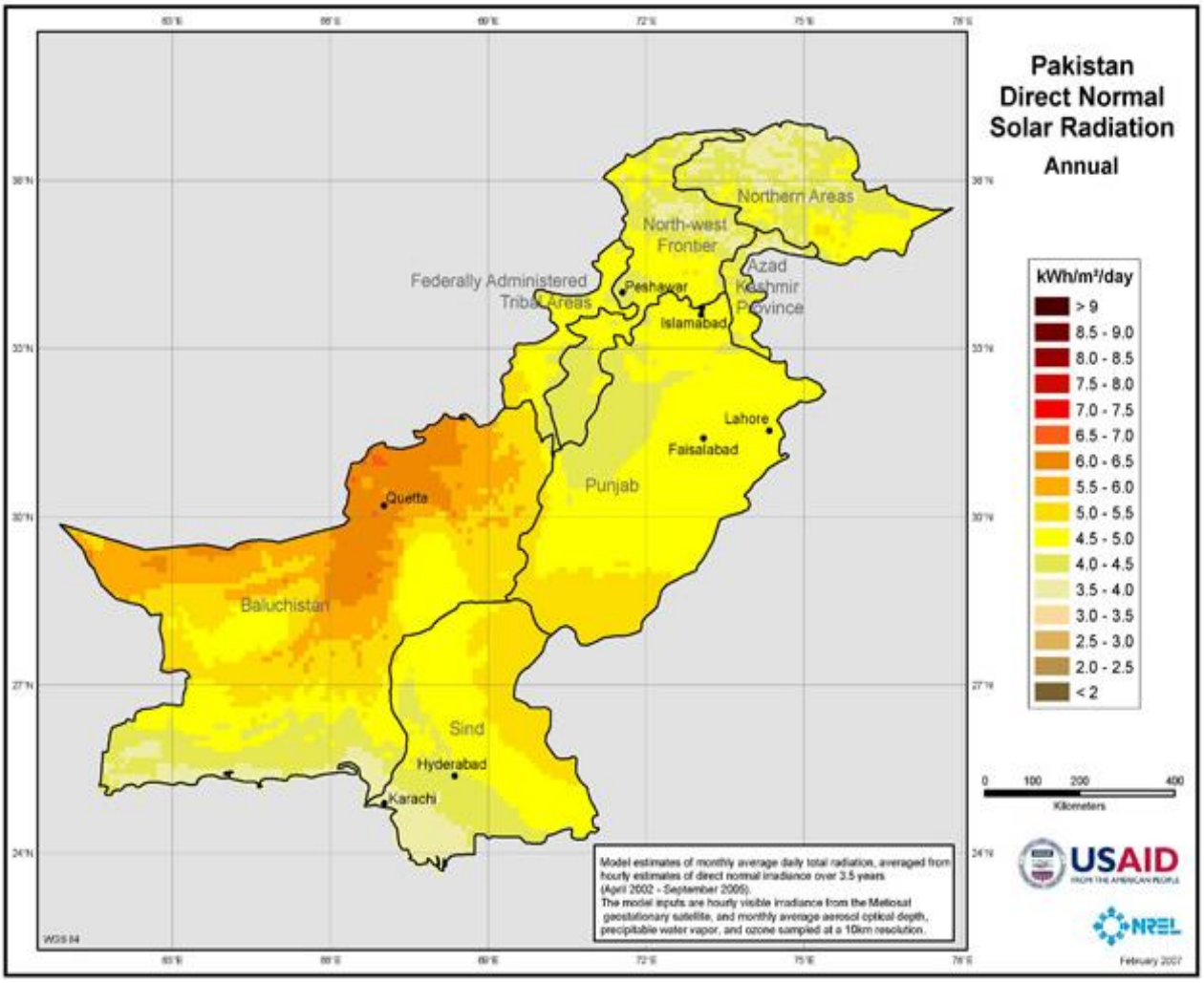

Figure 1-1: Power and Cell Temperature Comparison

1.5 Photovoltaic Cell

Photovoltaic (PV) cell is a standalone device which converts solar energy in terms of photons directly in to electricity (DC). Photovoltaic cell contains semiconductors that follow the photovoltaic effect. There are different type of semiconductors that are being used for PV cell that include monocrystalline silicon, polycrystalline silicon, amorphous silicon, cadmium telluride and copper indium gallium selenide.

1.6 Novelty and Contribution

- To minimize solar module cell temperature.
- To enhance the efficiency of photovoltaic cells.

1.7 Scope of Study

- Study of PV module structure
- The effects of external environment on working efficiency on PV cell
- Identification of sensitive layer/part in PV module
- Modeling of equivalent PV module by using CFD simulation software
- Development of modified PV module by adding a new layer
- Analysis of results for further optimization of newly added layer

2 LITERATURE REVIEW

In the following section, a brief literature review has been carried out for the analysis of cell temperature factor which affects the efficiency of the Photovoltaic PV modules. For the literature review, material from books, research journals and material on internet has been studied to analyze the research and for the development of experimental work related to cell temperature effects and an increase in conversion efficiency of PV cells by using different cooling systems.

In [2], a research was conducted to analyze the effects of temperature on PV cell and researcher tried to increase the cell conversion efficiency by adding an air layer. The duct was fabricated for utilization of fluid (wind) by natural convection through the photovoltaic module to reduce the cell temperature. It was stated that an increase in cell temperature per degree from its designed (rated) temperature reduces the efficiency about 0.5% from its rated efficiency (16%).

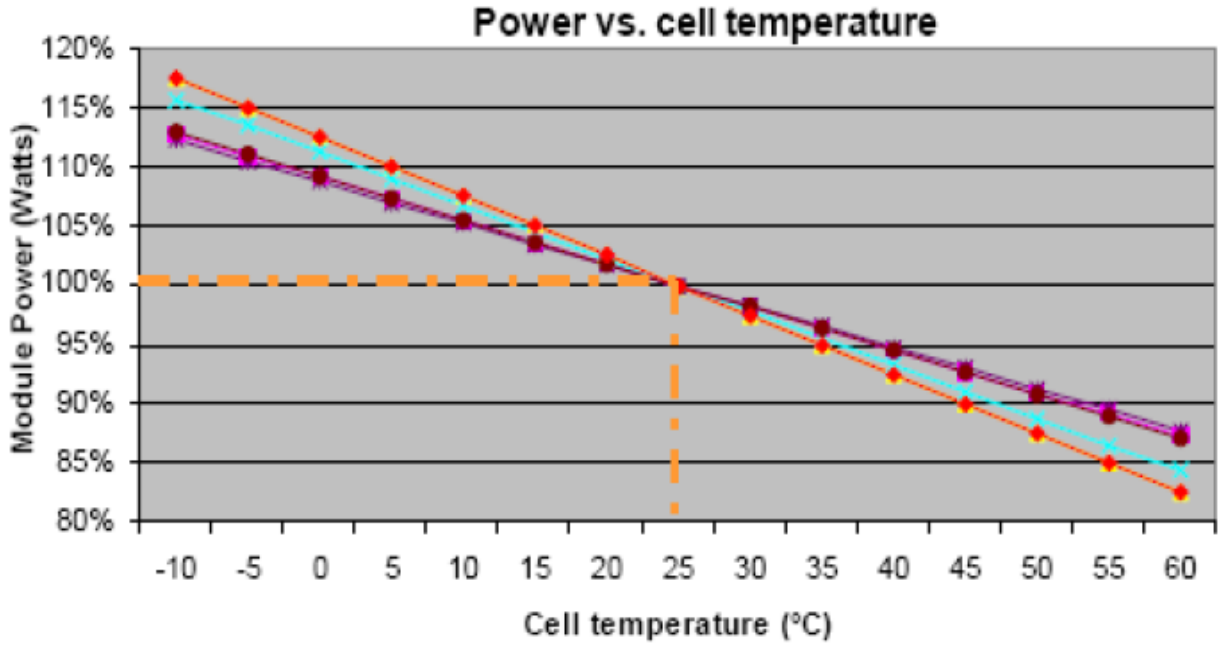

Figure 2-1: Power and Cell Temperature Comparison

Computational Fluid Dynamics (CFD) simulation was used out to analyze the heat dissipation and air flow behavior of modified solar module. The proposed design was simulated in Flovent

CFD software which provides the information about the pressure, temperature and air flow throughout the air gap of solar module. PV module was modified by introducing the gap between the solar cell and back cover (Aluminum sheet) as shown in figure given below.

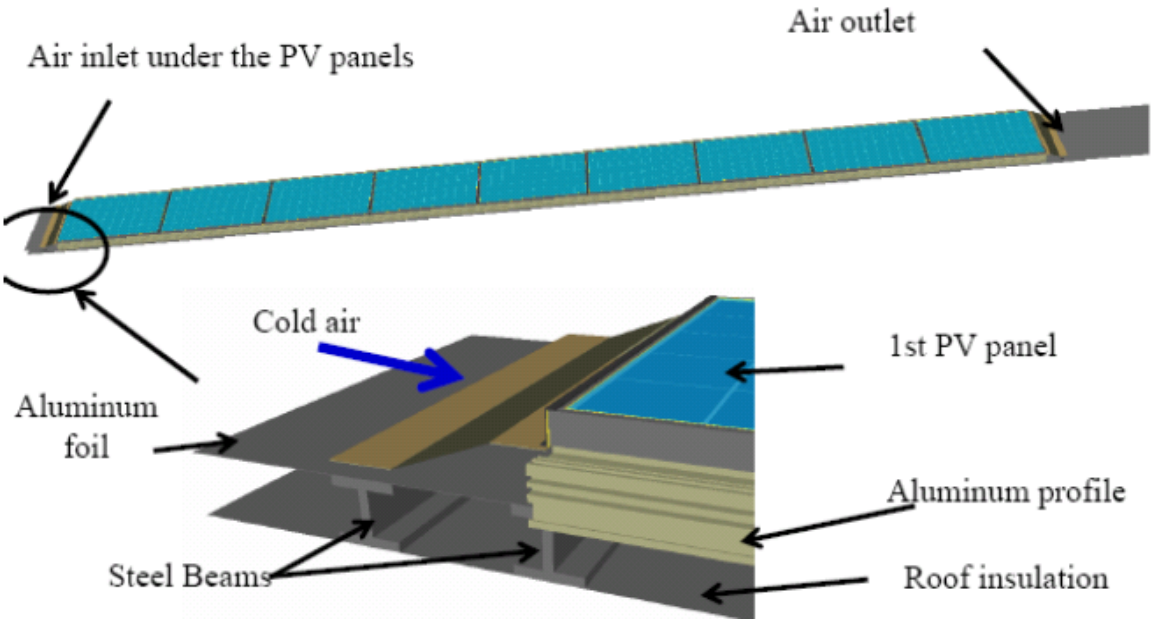

Figure 2-2: CFD Flovent analysis of Modified Solar Photovoltaic Module System

The simulation results showed that at ambient temperature of 25 ^{0}C to 37 ^{0}C, temperature in air gap was 60 ^{0}C which later was dissipated by natural convection of wind.

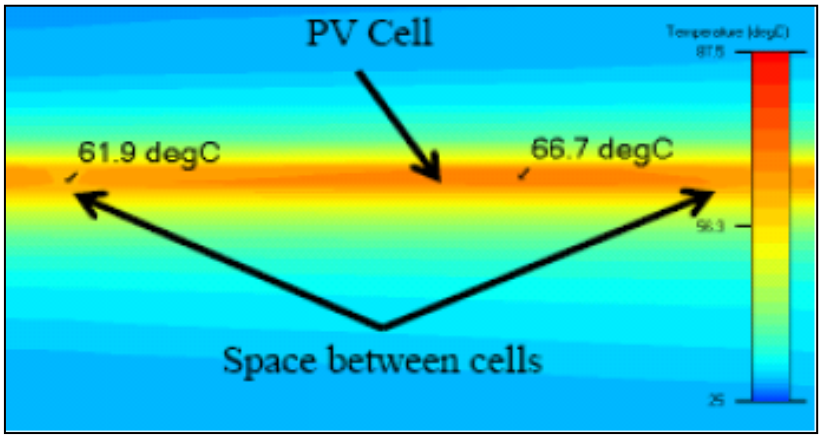

Figure 2-3: Air Temperature [2]

Another study was conducted in [3] to determine the efficiency loss with an increase of cell temperature. It is stated that in the summer, average ambient temperature of UAE reaches up to 42˚C which caused to increase the cell temperature up to 80˚C and this decreased power generation by 0.65% per Kelvin and conversion efficiency about 0.08%.

Computational Fluid Dynamics (CFD) study was carried out to modify the photovoltaic modules by introducing finned heat pipe arrangement for cooling purpose. Fined heat pipe was attached at the back of the photovoltaic module to reduce the cell temperature. The modified module structure is shown in figure 2-4.

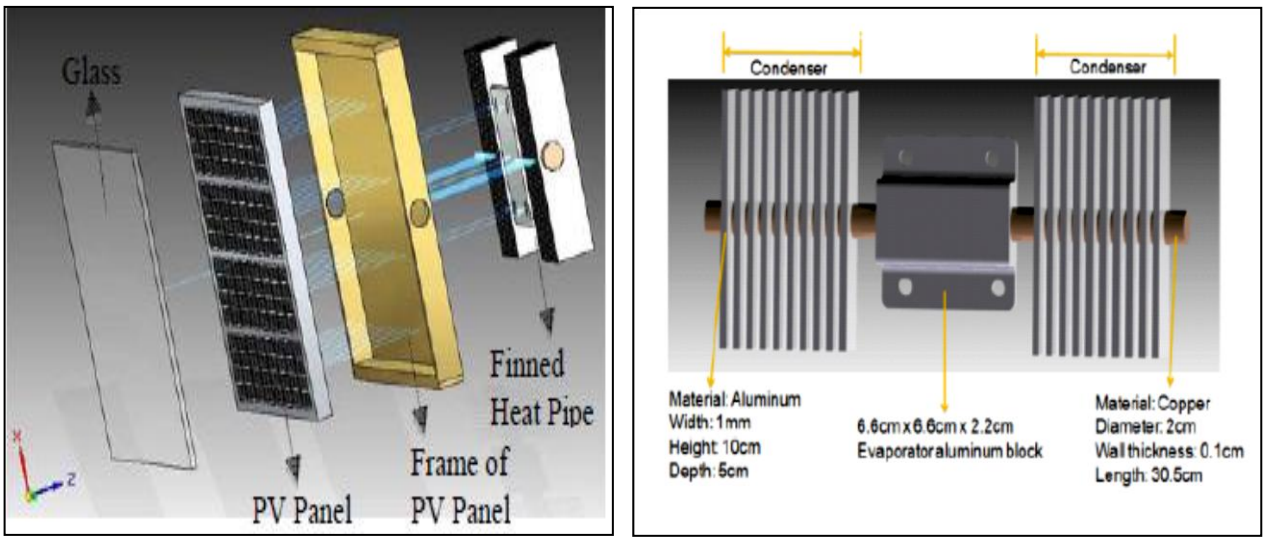

Figure 2-4: Proposed Photovoltaic Cell Arrangement

Aluminum blocks were fitted across the heat pipe and this was assembled by Boxford CNC machine. Finned heat pipe absorbs heat from the cell by conduction and then dissipates collected heat through natural convection from the ambient air.

The modification of PV Cell was done by CFD Simulation to analyze free-stream air flow and temperature contours by using GAMBIT, FLUENT Pre processor and ANSYS 12.1. All parameters were known through digital instruments and calculated cell temperature by using Ross Approximation.

The proposed finned heat pipe fabrication for cooling PV cells may contribute to maintain an efficiency and cell temperature in high rise temperature countries. It may be investigated for effective modification to generate both thermal energy and electrical energy.

It is observed that with the help of the finned heat pipe arrangement and natural convection (wind speed of 4.2m/s and temperature of 315K) the PV module has an operating temperature on the solar cells of 300K.

In another research [4] an experimental study was conducted to increase electrical power output of the PV cell. It was calculated that when PV module's cell temperature increases the voltage of module decreases about 0.4%/°C to 0.5%/°C

PV cell temperature can be reduced and maintained by flowing water over the surface of the Module. It cools down the surface temperature which reduces the entire cell temperature, because quick flow there will be a minimal increase in water temperature.

Figure 2-5: Water Flow Over the PV Modules by Nozzles

Approximately 2 l/min of water were spread through nozzles mounted on the module. Flow over the module improved the optical performance and operating temperature was reduced up to 22°C

simultaneously. Power output and cell temperature variations between the conventional and module with water film can be seen in below figures:

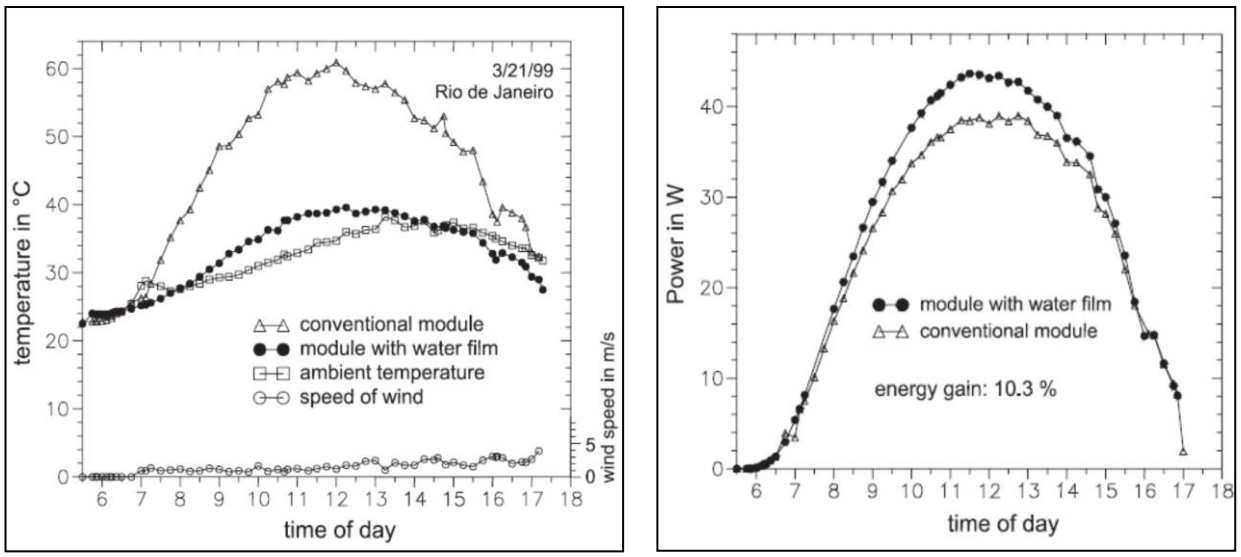

Figure 2-6: Cell Temperature and Power Output Comparison [4]

In [5], photovoltaic cogeneration module also known as solar duct was introduced, which produces both electrical and thermal energy. Study highlighted the facts of decreasing the rated efficiency of photovoltaic cells. This method was deployed to reduce the temperature that increases behind the module which reduces electrical output by 0.5%/°C above their rated designed temperature.

Photovoltaic cogeneration technology comprises of multifunction, conventional PV modules were fabricated with an addition of air duct at the back of the module. The air circulated through the duct which carried heat away from the module and this excess heat were gathered in the HVAC system where it is used to offset the heating load. This cogeneration process is also known as PV/T Photovoltaic / Thermal system

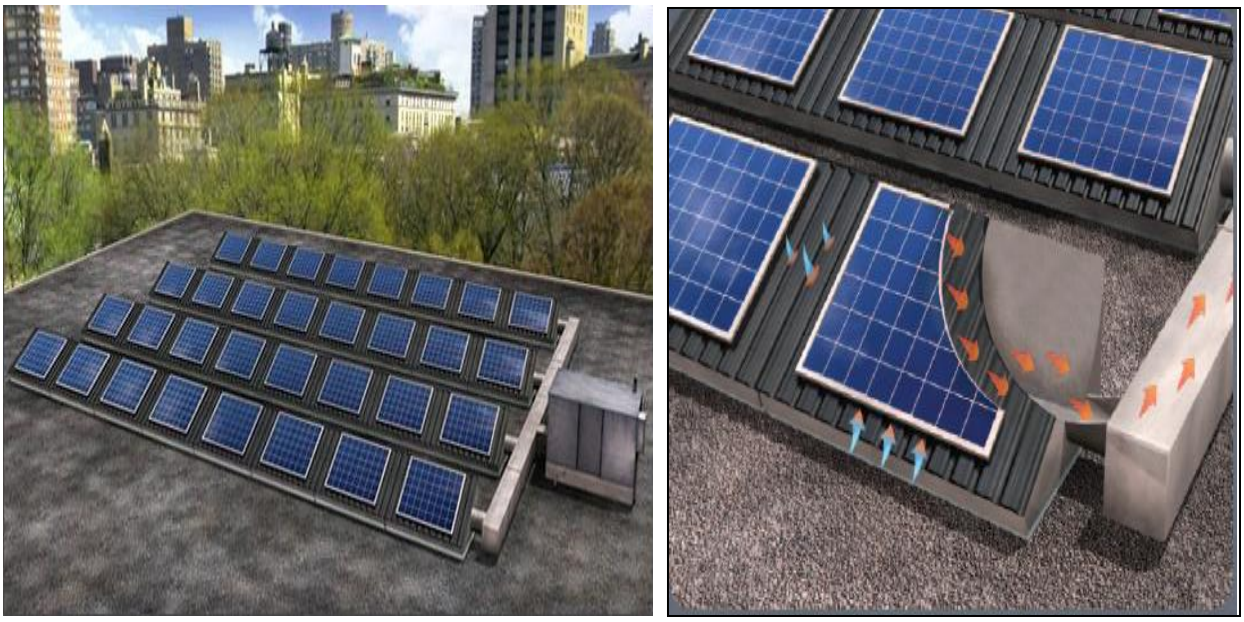

Figure 2-7: Solar Air Duct System (PV/T)

In another study [6], conventional photovoltaic cells were modified with cooling system by novel micro heat pipe. Author analyzed that an increase in cell temperature above their rated temperature may reduce the conversion efficiency of PV Module by 0.2% to 0.5%.

Heat pipe consisted of two sections: Evaporator and condenser. Evaporator was placed at back of the PV Module which was poured by liquid. Heat at the back of cell vaporized the liquid which were transferred to the condenser and the condenser section was cooled down by Air and water respectively. The heat Pipe transfers heat from solar module to air and water to reduces the temperature of PV module that improves the PV conversion efficiency. Air cooling and water cooling method were used to reduce cell temperature and compared with conventional Photovoltaic cell

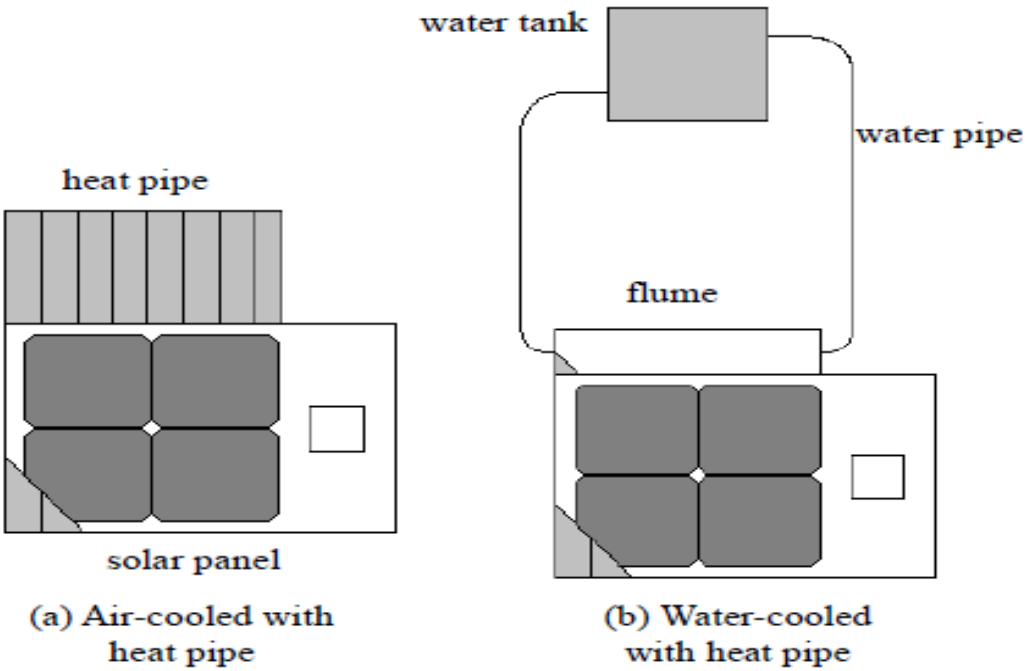

Figure 2-8: Cooling System of Solar (PV) Module

Air cooled PV cell as compared to conventional cell, the temperature of the cell using air cooling systems decreases up to 4.5˚C with an efficiency difference about 2.6% and water cooling system reduces cell temperature up to 8˚C with an efficiency difference about 3%. Maximum efficiency of about 13.5% can be achieved by water cooling system.

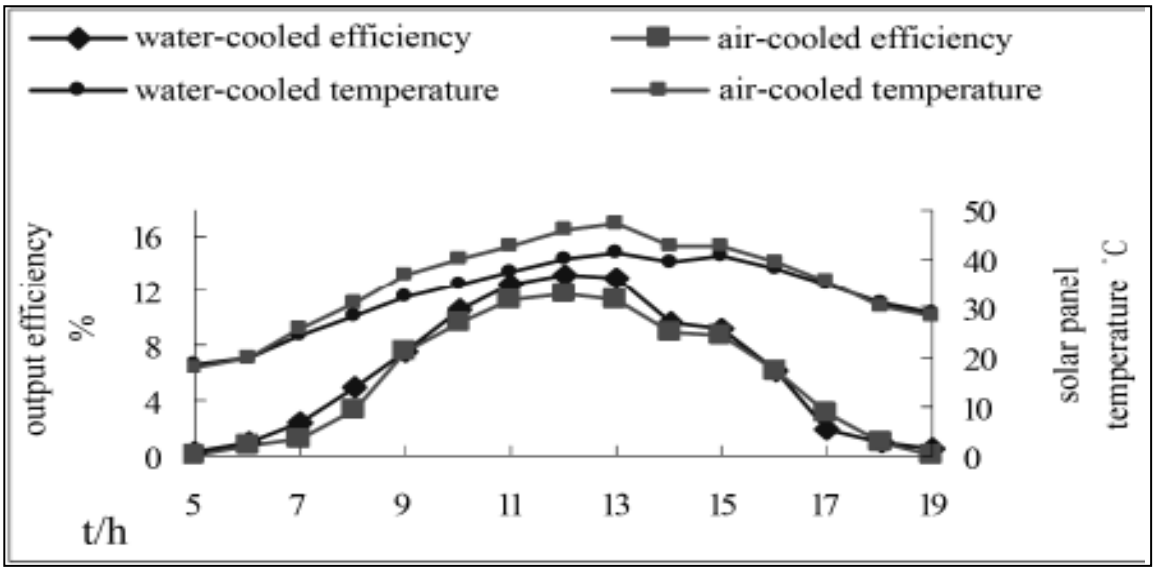

Figure 2-9: Photovoltaic cells with cooling system comparison

An experimental study [7] stated that the high temperature of PV cell can be cooled down through forced flowing water to improve the efficiency. PV Module was modified by assembling copper pipes at the back of cell. Maximally heat was expected to cool down by flowing water through copper pipes.

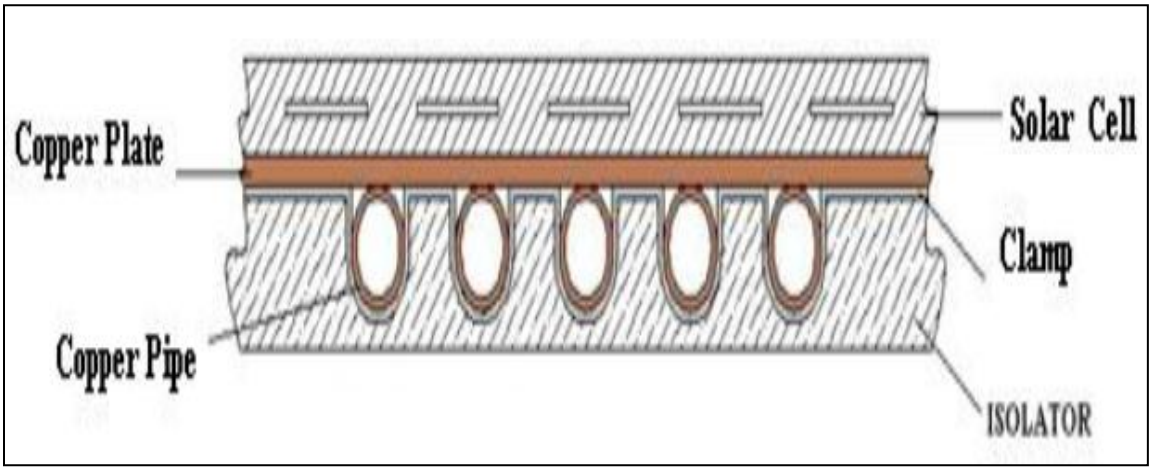

Figure 2-10: Water Cooled Photovoltaic cell

Water tank were placed over the cell for continuous flowing and this research shows that the increase in the flow rate of water may affects the cell temperature, surface temperature, power output and conversion efficiency of the PV module. Results show that an increase in flow rate caused decrease in surface and cell temperature. Research was carried out on different flow rates which shows that maximal temperature difference achieved on maximal given flow rate of 400 ml/min. cooling water temperature was increased up to 43˚C and this warm water can be used for domestic as well as commercial and industrial applications.

In [8], a detailed experimental research on Concentrating Photovoltaic (CPV) system have been carried out in which the Cell cooling were addressed as critical issue for CPV system, it was stated that the system temperature raises under high illuminations which reduces cell efficiency. Effective heat system should be required to cool down the cells.

The authors introduced the liquid immersion CPV dish system which comprised of two axis tracking dish concentrator. PV module were placed inside the glass pipe, electrode and thermocouple wires were fixed and covered by a stainless steel pipe to keep away the expose of wires into the densely ionized (DI) water poured in glass pipe.

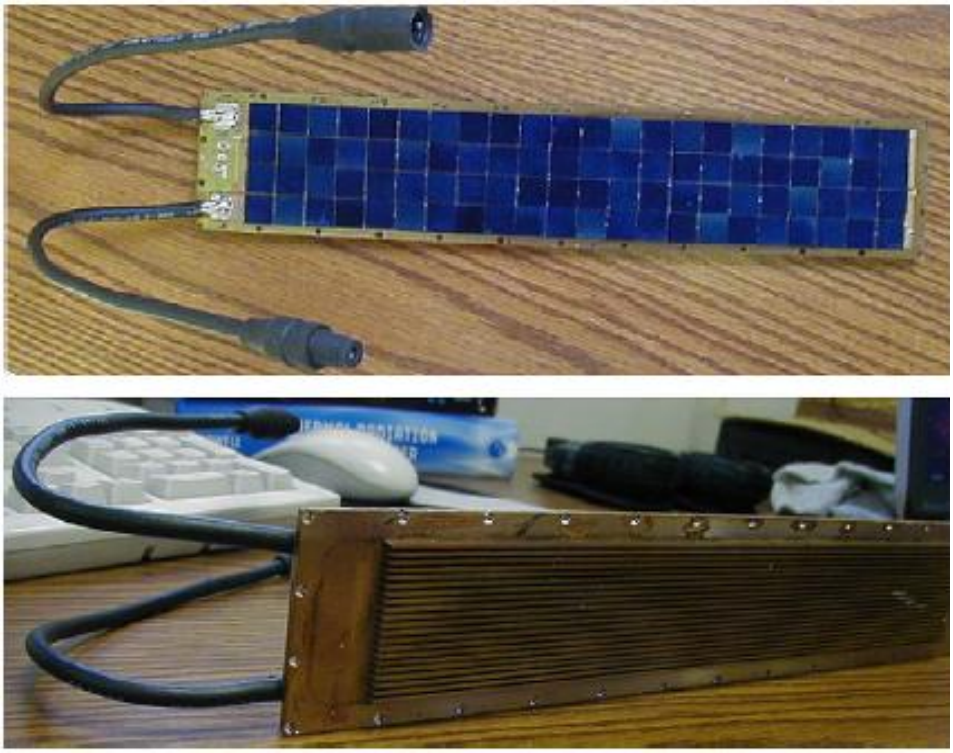

Figure 2-11: Cell module for Receiver assembly

DI water is circulated through the PV module for cooling purpose. Further heat is rejected from DI water to Tap water by using Heat Exchanger. DI water is an effective immersion medium because of high thermal capacity and low viscosity. The cooling ability of DI water is very favorable and module temperature can be maintained up to 45˚C at 950w/m^2 solar isolation, 17˚C ambient temperature and 30˚C water inlet temperature. But it has draw backs that electrical performance of the module may be affected after a long time immersion in the de-ionized water[8].

Figure 2-12: Liquid Immersion Concentrated Photovoltaic Module

In another research [9], it was expressed that an increase in cell temperature may produce more energy. The experiment was carried out in which first solar cell were kept in freezer to freeze it up to 10˚C then placed it in ambient air as the cell became warmer an increase in power was achieved till 24˚C. Then cell was also heated in oven till 100˚C, again solar cell was placed in normal ambient conditions. It was analyzed that as cell temperature decreases, this causes a slightly increase in voltage occurred and power output reached at highest when cell temperature till 24˚C. Through this experiment, it was proved that an increase in cell temperature above their rated temperature may reduce cell efficiency [9].

By [10], solar cell temperature effects on efficiency are described in detail. An increase in temperature reduces the magnitude of exponent in the characteristic equation. (Io) slightly increases with an increase in temperature and Net effect is the increase in temperature is inversely proportional to the open circuit voltage (Voc). Reduction in Voc with an increase in temperature is 0.50% / ˚C. [10]

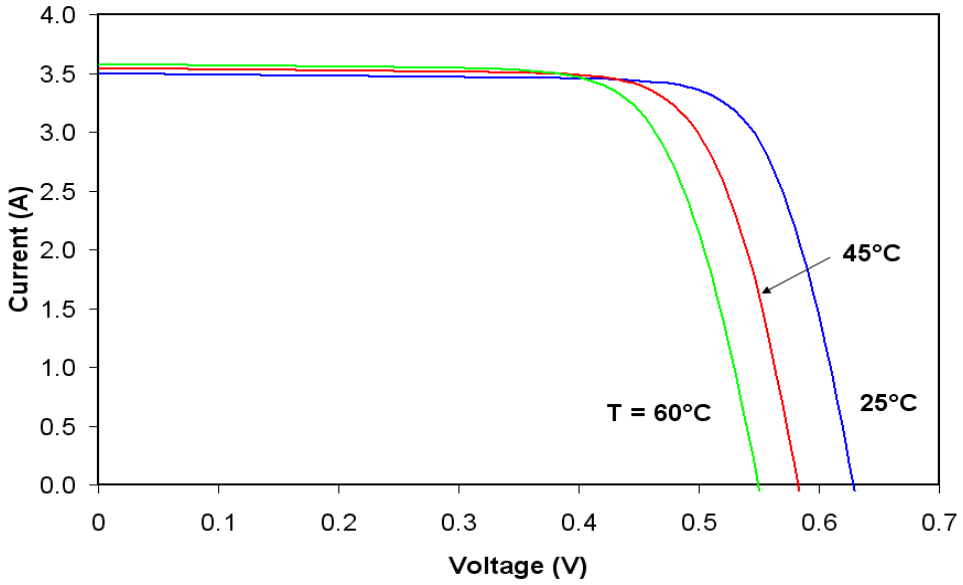

Figure 2-13: Temperature Effects on Current and voltage characteristics

An Italian researcher [11] stated that the cell efficiency and stability reduces in high rise temperature areas thus he introduced a solar cell coupled by micro heat exchanger at back of the cell. A prototype heat exchange is used with the simple design, in parallel to heat micro channels and the size of each channel is 12.5mm in length, 0.5mm width and with a height of 2mm. Aluminum material is used for top and bottom cover of heat exchanger, fins are pasted in the top cover and covered by bottom plate as shown in figure: 14, A highly thermal conductive grease is used to make good contact between the cell and heat exchanger pieces. As fluid applies to the heat exchanger, a sudden change in temperature profile was noted .

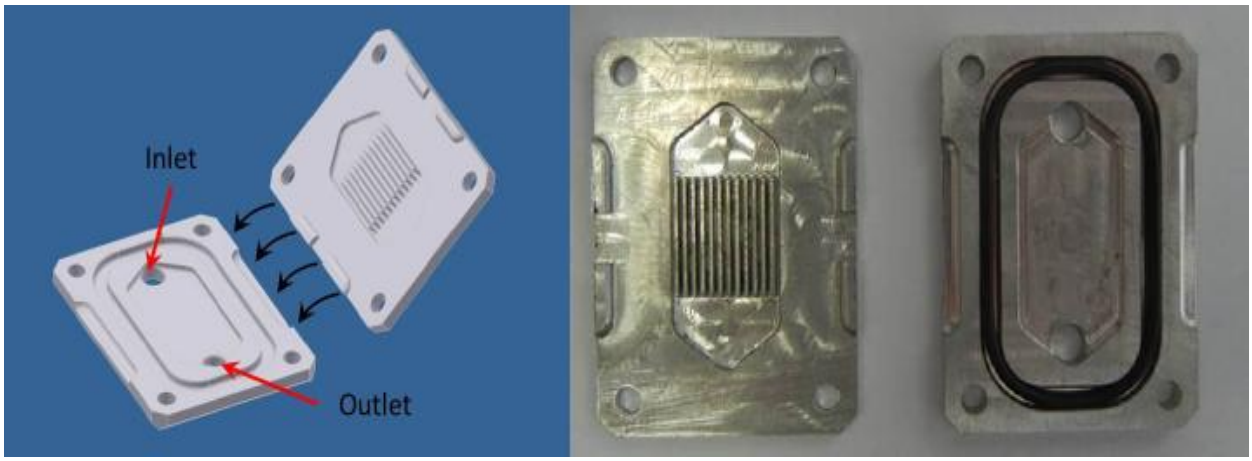

Figure 2-14: Geometry of the prototype heat exchanger

In [12], a study was carried out about the conversion efficiency of cell, a thermal system contains aluminum reservoir was designed and attached at the back of the PV cell to absorb heat to increase the conversion efficiency. The cooling reservoir with thickness of 1mm is bonded at the back of cell with a thermal paste. Aluminum material was chosen for reservoir because of its high thermal conductivity, low cost, easily available in market and feasible for in combination with solar cell material.

System was modeled at different thickness level of the reservoir in the COMSOL software and cold water flows at different flow rates inside the reservoir by forced convection and hence heat was carried out away from the cell in the water.

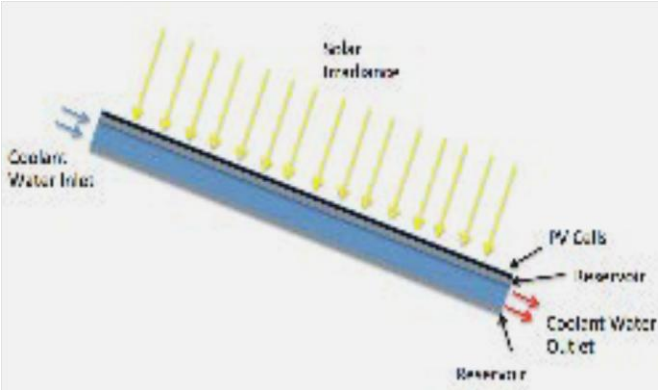

Figure 2-15: An Aluminum reservoir

In [13], hybrid Photovoltaic/Thermal (PV/T) system fabricated to increase the efficiency of the cell. Solar modules of total 220W capacity were used with deep cycle GEL type battery to store energy. An air duct was designed with an inlet and outlet and was attached at the back of the cell while fins are fixed inside the air duct to increase the heat transfer rate. Experiment took place by using active and passive cooling system. In order to utilize active cooling, DC blower was connected to the batteries to extract air from the surrounding and supplied it to the air duct. Whereas, passive cooling works without Blower.

Without active cooling, air is supplied to the duct in which resulted a slight change in temperature with an efficiency of 8-9%. By applying active cooling, an amount of temperature

decreases with an increase in efficiency upto 12%. Heat extracted from the PV module can be utilized in low temperature applications .

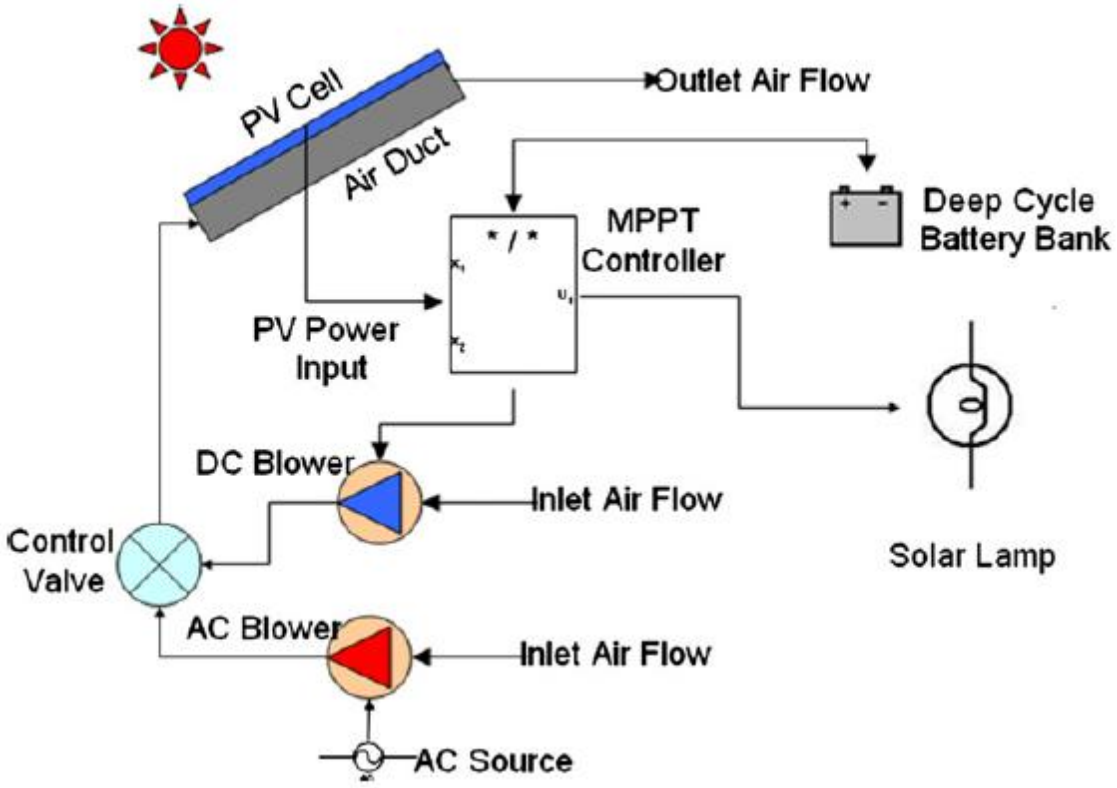

Figure 2-16: Schematic diagram of hybrid PV/T system

3 SOLAR PHOTOVOLTAIC TECHNOLOGY

Photovoltaic (PV) cell is a standalone device which converts solar energy in terms of photons directly in to electricity (DC). PV cell contains semiconductors that follow photovoltaic effect. There are different type of semiconductors are being used for PV, includes monocrystalline silicon, polycrystalline silicon, amorphous silicon, cadmium telluride and copper indium gallium selenide. Today PV is the rapid growing green energy technology for electricity production and also contributes to control the global warming. In this chapter; construction, working principle and behavior of solar PV technology has been described in detail.

3.1 Solar Photovoltaic Cell

Solar cell is an electronic device which converts sunlight (Sun emits photons/radiation through the thermo nuclear fusion reaction) directly into electricity. Solar photons contain high energy strikes on the solar cell surface which produces both a voltage and current. Photon absorption by the material raises the electrons energy state level and therefore it moves from solar cell to an external circuit[14].

Figure 3-1: Solar Cell

All types of PV cells use variety of semi conductors in the form of P-N Junction for energy conversion. PN junction is the boundary between the two types of semiconductor created by doping.

3.1.1 Semiconductor Materials

A semiconductor is a material whose electrical conductivity lies between the electrical conductivity of metal and insulator. A pure semiconductor is a poor electrical conductor but it has ability to change the conductivity by adding impurities and by the interaction of other phenomenon. The properties of the semiconductor vary with the variation of materials. Semiconductor material mostly comes from Group IV in a periodic table as well as it can be combination of materials that lye in Group III & V together and in Group II & VI together.

Semiconductor materials such as Silicon (Si), Cadmium sulphide (CdS), Gallium arsenide (GaAs) and Cadmium telluride (CdTe) can be used to fabricate solar cell. Semiconductors are divided in to two categories which are intrinsic and extrinsic. An **intrinsic** semiconductor is a pure semiconductor with low conductivity. A conductivity of semiconductor may easily be modified by introducing impurities in an intrinsic semiconductor. A process of adding impurity atoms to a conductor is known as **Doping** and the doped semiconductors are referred as **extrinsic** semiconductor.

When a crystal of pure silicon with four valence electrons is doped with atoms having five electrons (e.g. phosphorus, arsenic, antimony, etc) the doped crystal carries excess electrons which can move freely and thus silicon so treated termed as ***n-type*** **semiconductor**. If a pure silicon is doped with atoms having three valence electrons (e.g. boron, gallium, indium), a vacancy of one electron is created in the lattice, producing a hole with positive charge. So silicon treated makes a ***p-type*** **semiconductor**. p-type and n-type both are extrinsic semiconductor and have higher electrical conductivity than the pure material.

In semiconductors, atoms are bonded together to form a uniform structure. Each silicon has four valence electrons, which are shared with the surrounding atoms to form a covalent bond. Figure in below shows the schematic representation in which each atom shares two electrons with another atom to form a covalent bond[14].

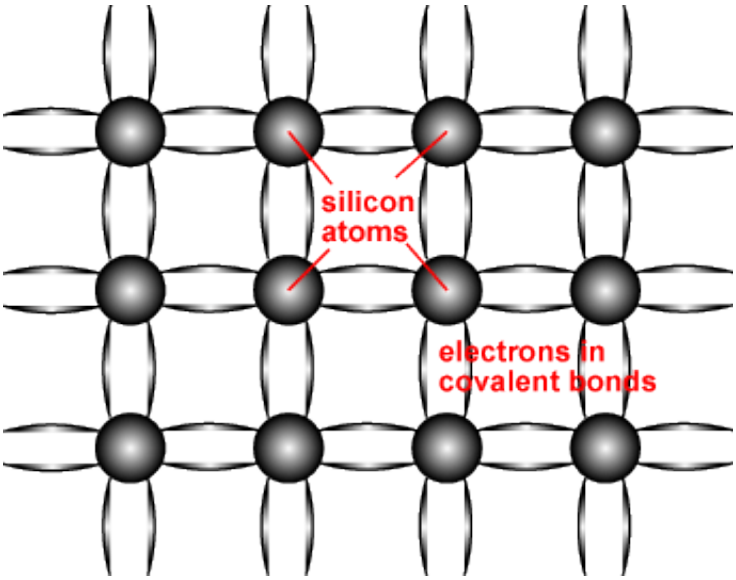

Figure 3-2: Schematic structure of semiconductor

3.1.2 Energy Band Gap

Band energy of a solid is the energy range of an electron that may have in the solid. In a semi-conductor, electrons may stay in one of the two energy band, conduction band or valence band. The conduction band has high energy level electrons but not fully occupied, while the valence band has lower energy level but fully occupied.

The gap between the two bands is called energy band or the energy level that differs between two bands is called energy band gap (Eg). No electron can exist in this region. Energy band gap is the minimum energy requirement for movement of electron from valence band to conduction band[15].

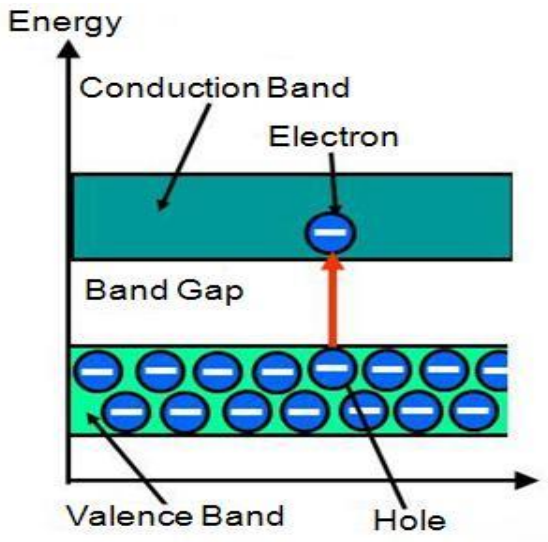

Figure 3-3: Energy Band Gap

As shown in following figure, insulators have large band gap, semiconductors have small band gap, while conductors have very small band gap or none. The valence and conduction band overlap in the conductor.

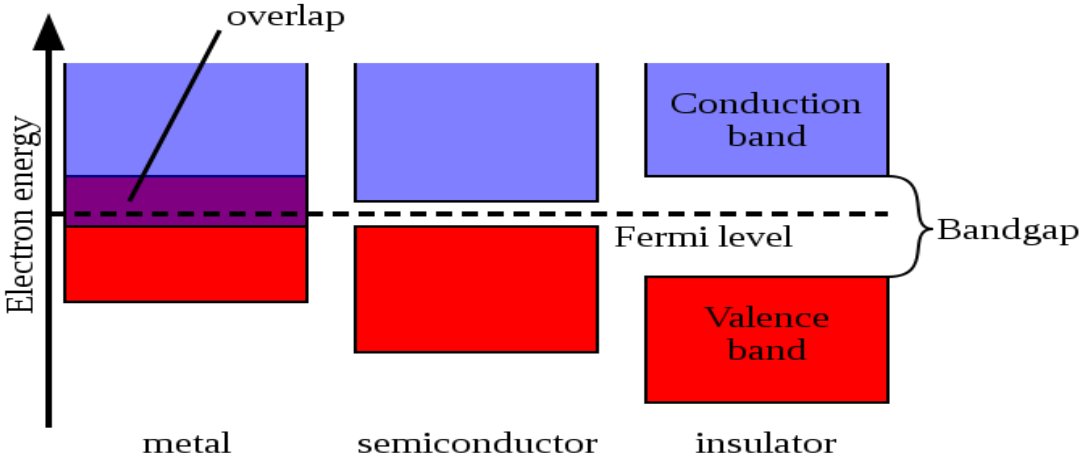

Figure 3-4: Band gap of difference material

The temperature dependence of the energy bandgap has been experimentally determined which is given below:

$$E_g(T) = E_g(0) - \frac{\alpha T^2}{T + \beta}$$

Where Eg (0), α & β are the fitting parameters and having different values for difference semi conductors[15].

3.1.3 PN Junction Formation

When semiconductor, doped with a donor impurity electrons in the conduction band, it becomes n-type material. When semiconductor, doped with an acceptor impurity, it becomes p-type material. When p-type and n-type are joined a junction is formed.

When the n-type material is made in contact with a p-type material, the electrons in n-type part move towards the holes in p-type materials. Hence the n-type becomes positive and p-type becomes negative. This diffusion process will continue until the flow of electrons and holes in the junction is in constant equilibrium conditions. An electric field is produced at the depletion region of a junction which sweeps electrons out and in results voltage in the junction is developed.

Forward bias occurs when the positive voltage is applied across the positive junction and this cause to decrease the electric field and reverse bias occurs when negative voltage is applied to the positive junction[15].

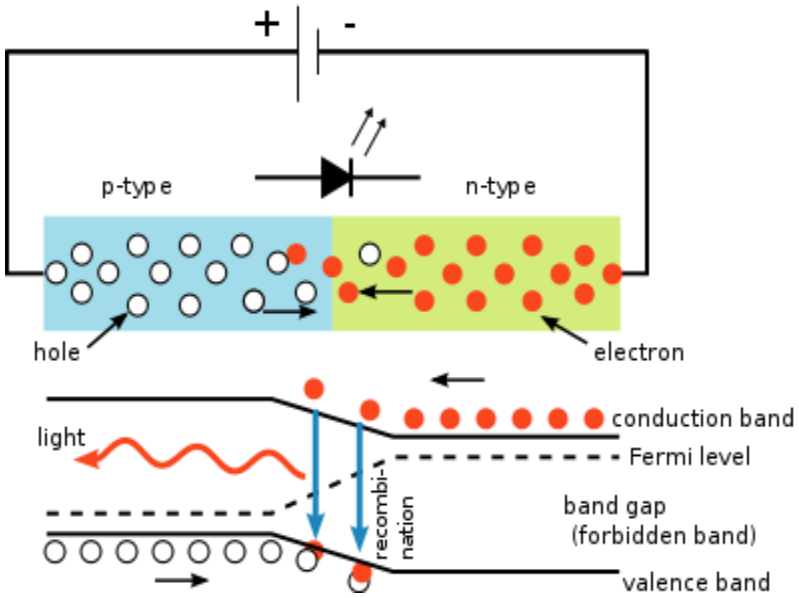

Figure 3-5: PN Junction Overview

3.2 Solar Photovoltaic Modules

Solar PV module is a device comprised of PV cells sealed by environmental protective materials. Combination of modules is known as the solar PV module as well as the combination of solar modules is known as Solar PV Array.

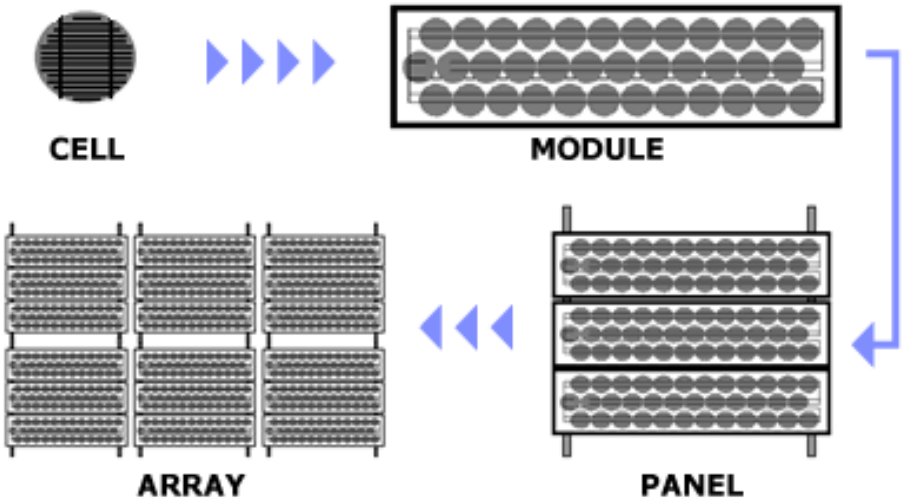

Figure 3-6: Schematic Diagram of Solar cell, module, module and array

In a PV module, cell is wired in parallel to produce the desired current and in series to produce the desired voltages. The module is encapsulated with tempered glass at the front surface, and a protective material and waterproof surface on the rear. The edges are sealed and there is often an aluminum frame holding it all together in a mountable unit. On the back of the module is a junction box [14].

3.2.1 Components of Photovoltaic Module

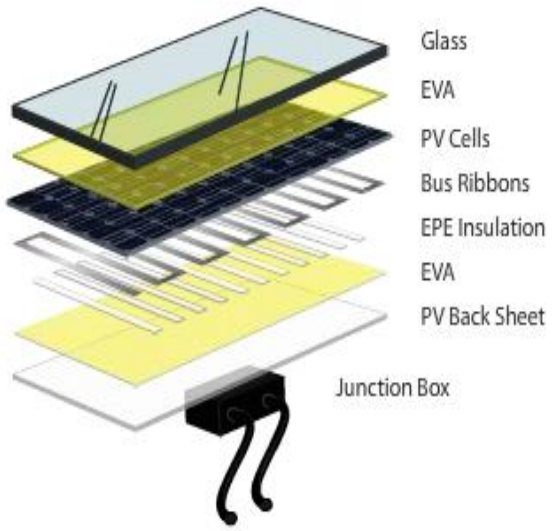

Figure 3-7: Main components of Solar Module

Glass is the transparent outer layer used to protect the solar cell from environment and only allowing light energy to pass through.

EVA (Ethyl Vinyl Acetate) is a thermoplastic polymer used to encapsulate (like capsule) the solar photovoltaic cell.

PV (Photovoltaic) Cell is made up of Silicon that converts solar radiation energy into electrical energy. Solar photons strikes on the surface of cell by passing through the glass and EVA layer as shown in above figure, therefore electrons comes in action and move throughout circuit .

Bus Ribbon is an external path which carries out electric current throughout the solar module.

EPE is a laminate with dielectric strength that act as an insulator like as backsheet.

Backsheet is used to protect the entire components of photovoltaic modules from UV, moisture and weather. It is even internally block the heat convection from the solar cell that reduces the efficiency of solar module. It is also used as insulation of electric load up to 1000VDC.

Aluminum and Tedlar Pet Tedler (TPT) is used as back sheet of Solar PV module. TPT is the polyvinyl fluoride (PVF) Polymer used as the back sheet due to its unique properties and superior protection against the elements. Weather, moisture & UV resistance. It is strong and durable adhesion, mechanical tough solution and chemical resistance.

3.3 Solar Cell Parameters

3.3.1 Open circuit voltage (Voc) & Short circuit current (Isc)

Open circuit voltage (Voc) is the electrical potential difference between the two terminals of device that disconnected by a circuit. Voc is the maximum voltage available at zero current in the solar cell.

$$V_{OC} = \frac{nkT}{q} \ln\left(\frac{I_L}{I_0} + 1\right)$$

An equation of Voc at I=0

Where:

n = Ideality Factor = 1

k = Boltzmann Constant = 1.38 x 10^{-23} Joule/K

q = Electron Charge = 1.6 x 10^{-19} Coulombs

T = Temperature

I_L = Light Generated Current

I_0 = Dark Saturation Current

Short circuit current (Isc) is the current of the solar cell when voltage across the solar cell becomes zero.

$$\mathbf{I = I_s\,[exp\,(qv/kT) - 1] - I_{ph}}$$

OR

$$\mathbf{I = I_s\,[exp\,(V_a/V_t) - 1] - I_{ph}}$$

Where $kT/q = V_t$ is the thermal voltage

Saturation Current (**Is**) of the diode is the current which flows in the reverse direction when voltage in diode becomes less than zero (Vd) due to minority carriers. It also known as the reverse saturation current. The value of **I**s of Silicon is 10–10 ~ 10–12. **I**s increases with an increase in Temperature and decreases with an increase in quality of material. [15]

Photo Current (**I_{ph}**) = **- Isc** (photocurrent is the maximum current flow in a reverse direction at Va=0)

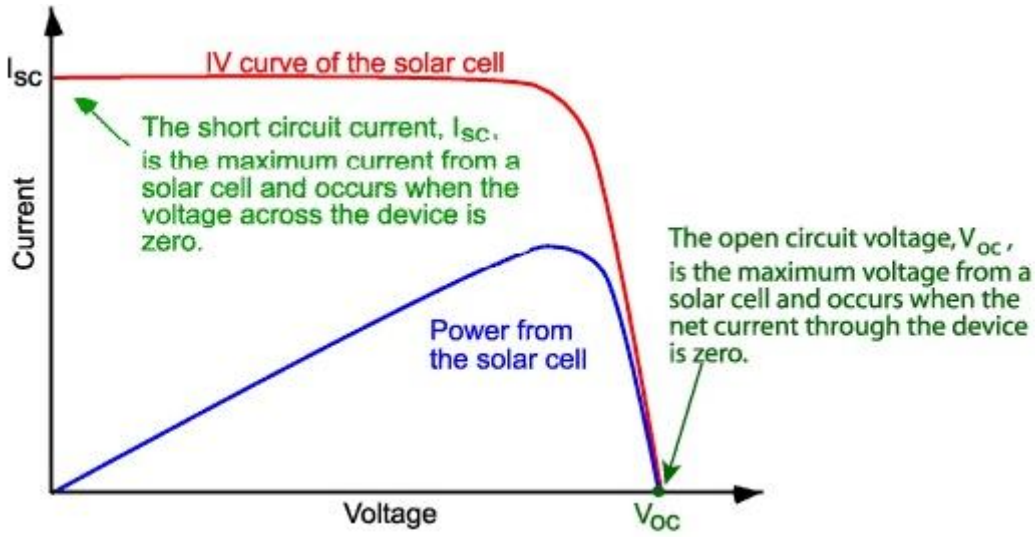

Figure 3-8: IV Curve of Solar Cell

3.3.2 Efficiency

Efficiency of solar cell is defined as the ratio of electrical power output to the energy that exhibits from the sun. Efficiency of the cell depends on some environmental conditions like as spectrum and intensity of sun light and the temperature of the solar cell. Terrestrial solar cells are measured under AM1.5 conditions and at a temperature of 25°C. Solar cells intended for space use are measured under AM0 conditions[15].

$$\eta = P_{out} / P_{in} = P_{max} / P_{in}$$

$$P_{in} = S \times A_c$$

P_{in} is the product of solar intensity (w/m^2) and the area (m^2) covered by solar module.

$$P_{max} = V_{mp} \times I_{mp} = V_{oc} \times I_{sc} \times FF$$

P_{max} is the maximum electrical output of the cell. P_{max} is directly proportional to the efficiency of the cell. Therefore the efficiency decreases with the decrease in P_{max}

Hence the final equation of the cell will become:

$$\eta = V_{oc} \times I_{sc} \times FF / S \times A_c$$

V_{oc} = Open Circuit Voltage

I_{sc} = Short Circuit Current

V_{mp} = Maximum Power Voltage

I_{mp} = Maximum Power Current

FF = Fill Factor (Ratio of maximum power to the product of V_{oc} & I_{sc})

S = Solar Intensity (w/m^2)

A_c = Cross sectional area of the cell

3.4 Efficiency losses

Photovoltaic cell plays a key role in the home energy market. It converts about 16% of energy captured from the sun into the electricity. But use of photovoltaic cell is limited because of its high cost and low efficiency.

The overall performance of the solar cell varies according to different irradiation and temperature. Solar irradiance is the power density per unit area of sunlight that strikes on the surface of the earth, therefore the received power by PV module changes with the change in solar irradiance over time of day.

When the temperature increases, the reverse saturation current increase (rate of the generation of photons increases) and this quickly reduce the band gap. Consequently, this leads to small changes in the current changes, but large in voltage.

3.5 An analysis of temperature effects on Solar Photovoltaic Module

An analysis of temperature effects on solar PV module has been carried out to understand the relation of an increased ambient and cell temperature with the efficiency of the cell. Therefore general parameters of a 10W polycrystalline solar module were choose to calculate the below given parameters. The parameters and calculations of solar module are given in **Annexure 1.**

3.5.1 Cell Temperature

Ambient temperature is directly proportional to the cell temperature. Therefore an increase in ambient temperature and solar intensity will increase the solar cell temperature[15].

$$T_{Cell} = T_{Air} + \frac{NOCT - 20}{80} S$$

Normal operating cell temperature (NOCT) is 25˚C and S (solar intensity) is 1000w/m^2 at STC level of 10W recommended solar module.

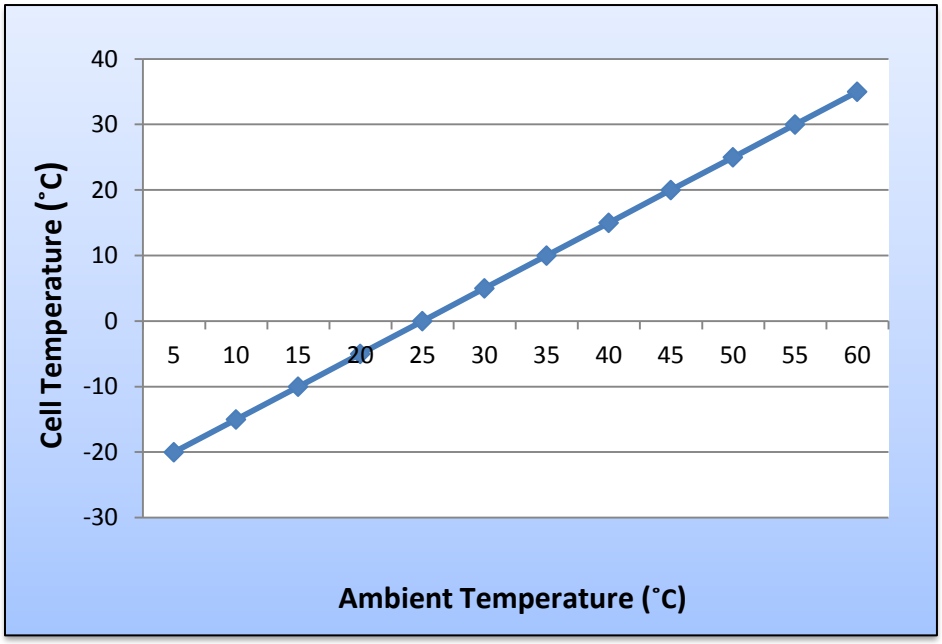

Graph 3-1 : Graphical Representation of Ambient Temperature & Cell Temperature

3.5.2 Energy Band Gap

Band gap is a major factor to determine electrical conductivity of a solid. Insulators have large band gap, Semiconductors have small band gap, while conductors have very small band gap or none. The valence and conduction band over laps in the conductor.

A semiconductor behaves like as insulator at zero band gap but allows thermal excitation of conduction band at temperatures below than its melting point. The bandgap energy of semiconductor tends to decrease as temperature increases. This behavior can be better understood if one considers that the interatomic separation increases when the amplitude of atomic vibrations increases due to increased thermal energy. This effect is measured by the linear expansion coefficient of a material.

The temperature dependence of the energy bandgap has been experimentally determined which is given below:

$$E_g(T) = E_g(0) - \frac{\alpha T^2}{T + \beta}$$

	Germanium	Silicon	Ga As
Eg(0) [eV]	0.7437	1.166	1.519
α [eV/K]	4.77 x 10-4	4.73 x 10-4	5.41 x 10-4
β [K]	235	636	204

Where Eg (0), α & β are the fitting parameters and having different values for difference semi conductors [15]:

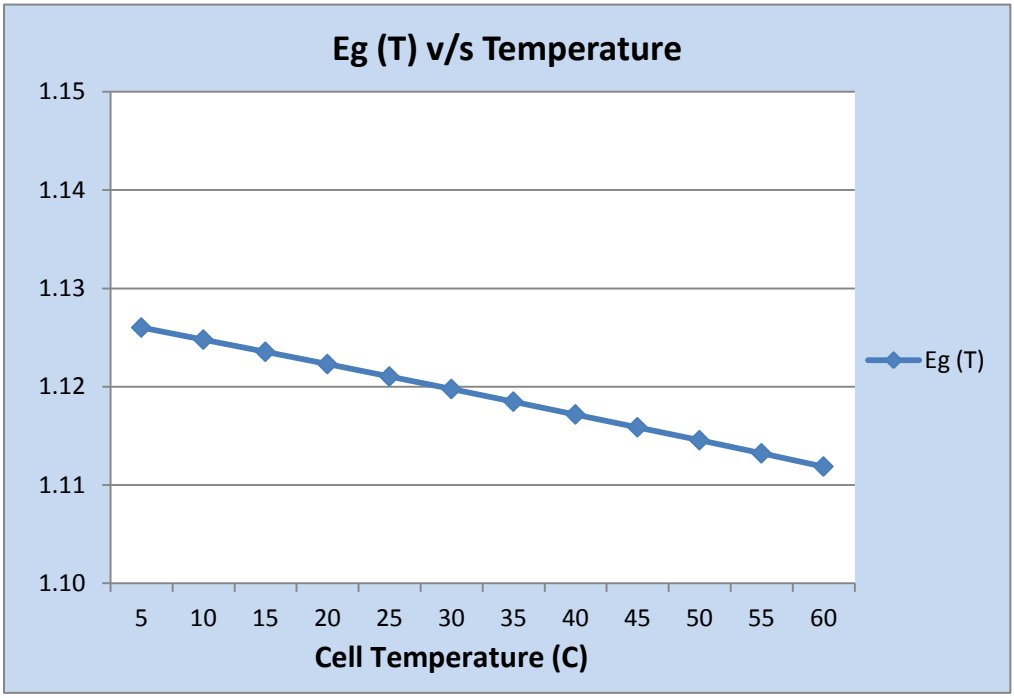

Graph 3-2 : Graphical Representation of Energy Band Gap & Cell Temperature

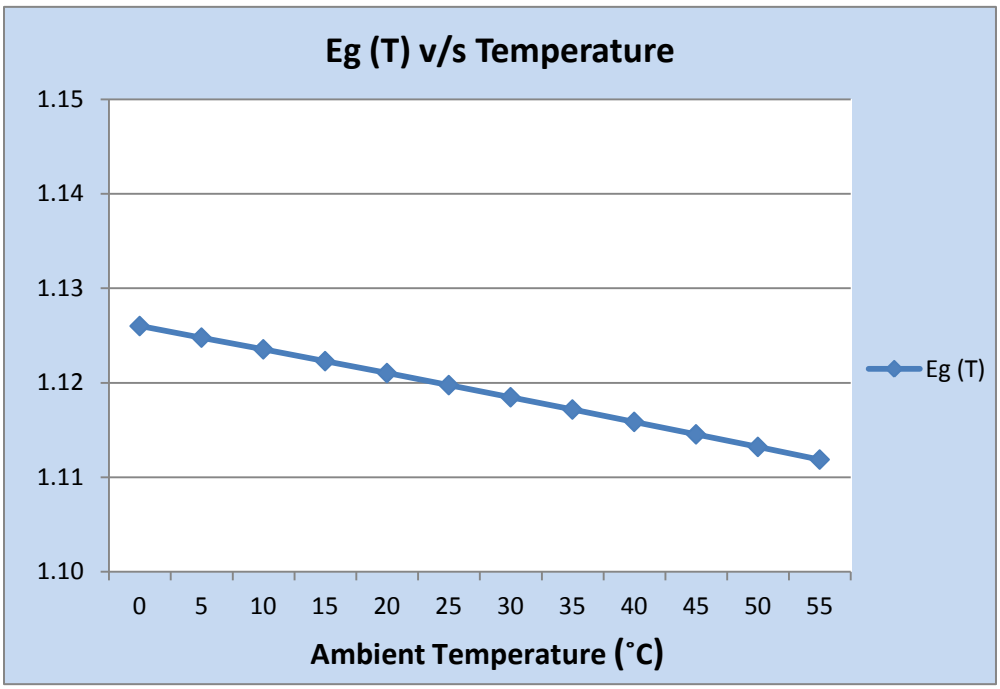

Graph 3-3 : Graphical Representation of Energy Band Gap & Ambient Temperature

The Graphical representation of the relationships of Energy Band Gap with Temperature shows that the band gap will shrink with an increase in ambient and cell temperature.

3.5.3 Voc & Isc

A graphical analysis of Temperature with Voc and Isc shows that an increase in temperature will reduce the Voc (open voltage current) and increases the Isc (short circuit current).

Voc & Isc were calculated by the given formula of thermal expansion:

$$V_{oc} = V_{oc\ stc}\,[1- (\beta \Delta T_{cell})]$$

$$I_{sc} = I_{sc\ stc}\,[1+ (\alpha \Delta T_{cell})]$$

$$\Delta T_{cell} = T_{cell} - T_{cell\ stc}$$

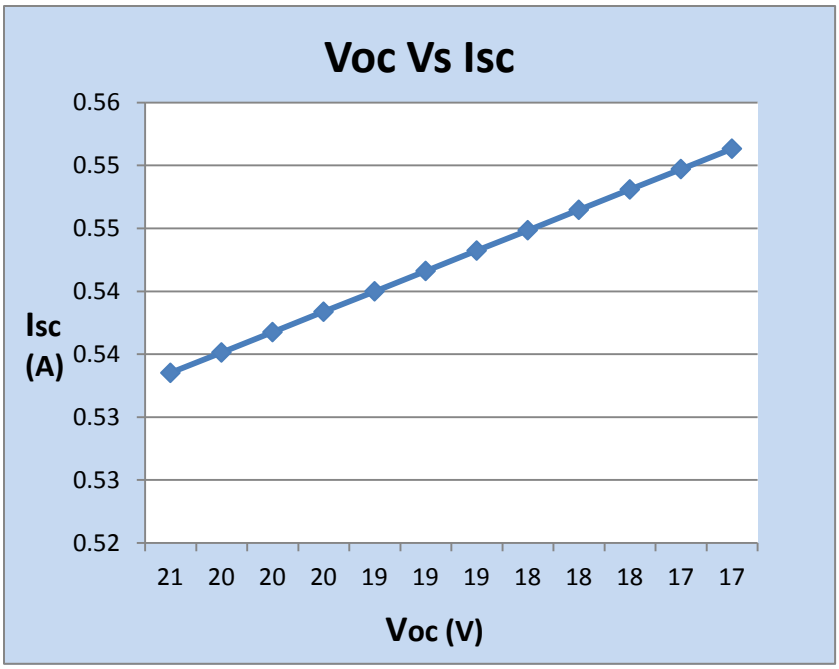

Graph 3-4 : Graphical Representation of Isc & Voc

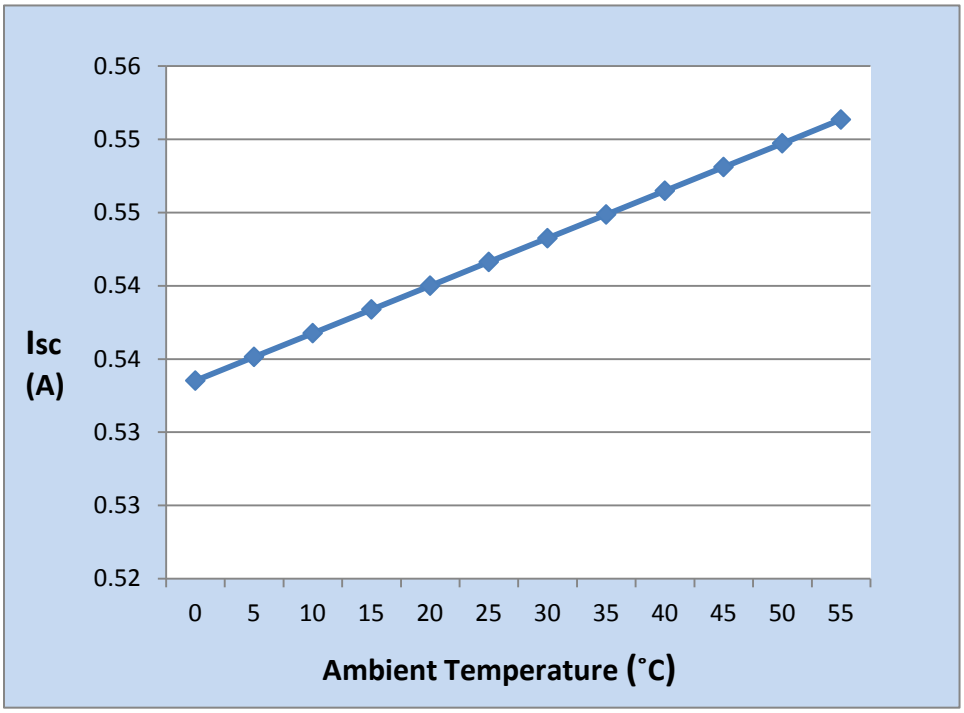

Graph 3-5 : Graphical Representation of Isc & Ambient Temperature

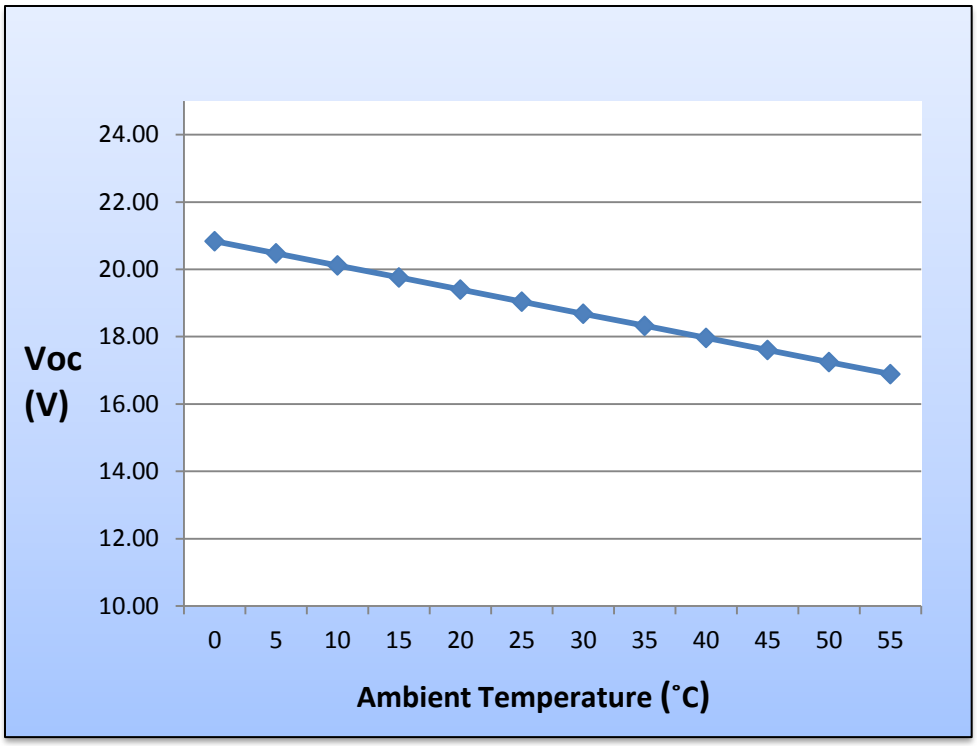

Graph 3-6 : Graphical Representation of Voc & Ambient Temperature

3.5.4 Efficiency

An increase in temperature will reduces the maximum power and efficiency of the solar cell. These were calculated by the following formula:

$$P_{max} = V_{mp} \times I_{mp} = V_{oc} \times I_{sc} \times FF$$

$$\eta = V_{oc} \times I_{sc} \times FF / S \times A_c$$

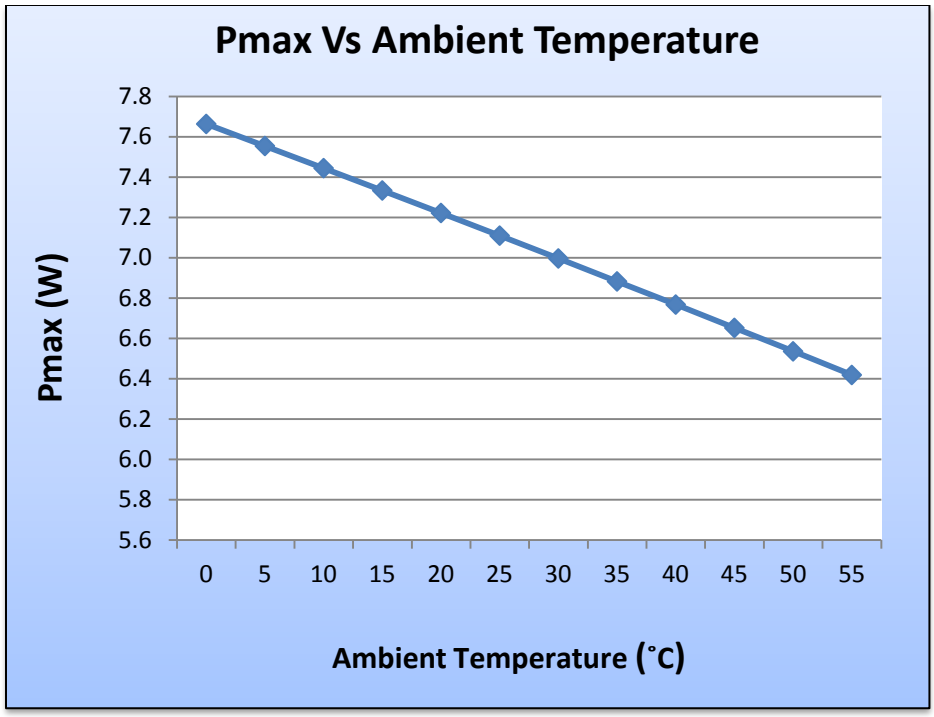

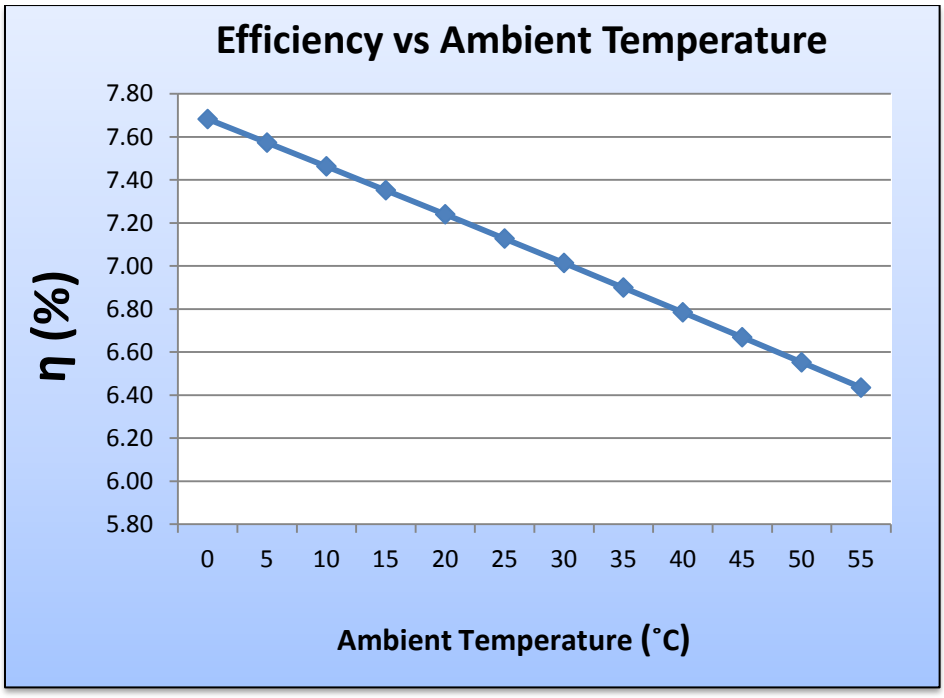

Graph 3-7 : Hence decrease in Power and efficiency can be shown in above graphs

4 PRACTICAL CONSIDERATIONS

4.1 Solar PV Module Specifications

Electrical Parameters at Standard Test Conditions (STC):

Power Output Pmax = 10W

Module Efficiency (η) = 10%

Voltage at Pmax (Vmpp) = 17.3V

Current at Pmax (Impp) = 0.58A

Open Circuit Voltage (Voc) = 21.3V

Short Circuit Current (Isc) = 0.66A

Irradiance = 1000 W/m^2

Cell Temperature = 25˚C

Temperature coefficient of Isc = α = 0.06%/°C

Temperature coefficient of Voc = β = - 0.37%/°C

Temperature coefficient of Pmax = γ = -0.45%/°C

Electrical Parameters at Normal Operating Cell Temperature (NOCT):

Power Output Pmax = 7.3W

Module Efficiency (η) = 7.2%

Voltage at Pmax (Vmpp) = 15.7V

Current at Pmax (Impp) = 0.46A

Open Circuit Voltage (Voc) = 19.4V

Short Circuit Current (Isc) = 0.54A

Irradiance = 800 W/m^2

Ambient Temperature at 1m/s = 25˚C

4.2 Solar PV Module dimensions

Length = 350mm

Width = 285mm

Height = 25mm

4.3 Modified Solar PV Module

The modification of conventional PV module is based on the experimental investigation of solar module cooling by a novel micro heat pipe array [6].

Parts:

a) Glass
b) EVA upper (Ethylene-Vinyl Acetate)
c) Cells
d) EVA lower (Ethylene-Vinyl Acetate)
e) Flat Plate heat Pipe
f) Thermal insulation (TPT)

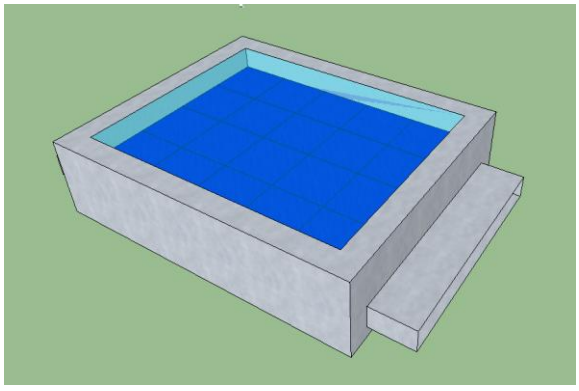

Figure 4-1: Modified PV Cell

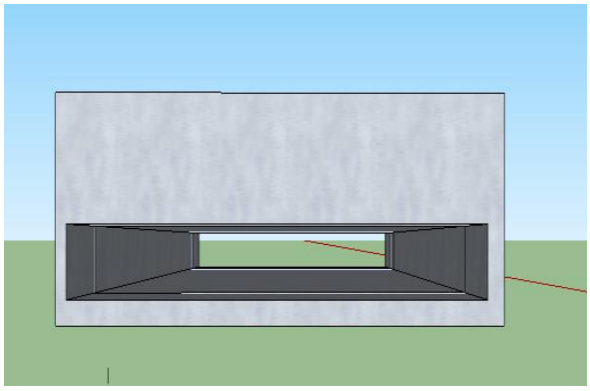

Figure 4-2: Air Duct Modified PV Cell

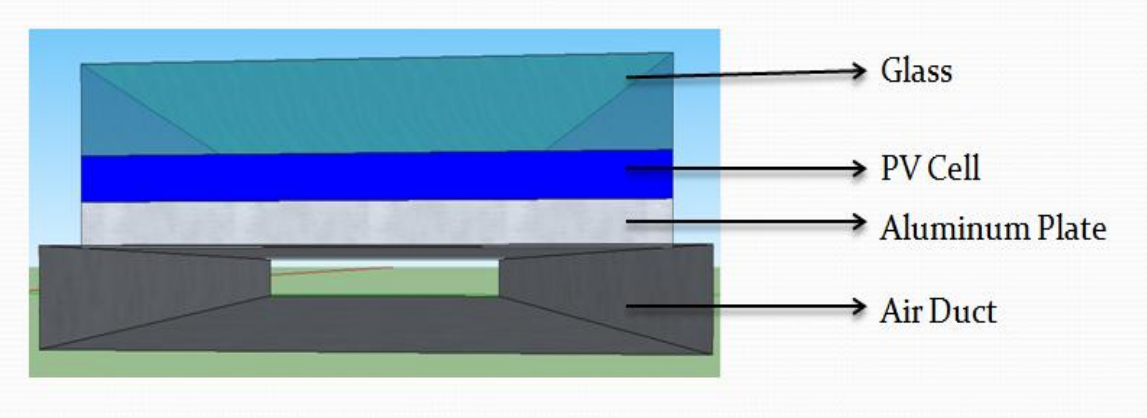

Figure 4-3: Modified PV Cell Structure

Micro plate heat duct made of aluminum have been used to modify commercial solar module. Silica Glue/Caulk used to paste the micro plate heat duct on the back of the PV cell as show in above Figure 4-3 and also ensure that the heat pipe contact closely enough to cell, at last thermal insulation used to reduce heat losses.

Heat in the cell dissipated away from the PV cell through the air duct, uninterrupted supply of air through duct reduces the temperature of PV module that enhances the PV conversion efficiency. Differences in results of cooling as compared with conventional Solar Module are further discussed in the next chapters [6].

Micro plate heat duct dimensions:

Length = 300mm, Width = 235mm & Height = 3mm

4.4 Materials and physical properties

S.No	Material	Thickness **mm**	Density **Kg/m^3**	Sp. Heat **j/kgK**	Thermal conductivity **w/Mk**
1	Glass	3.2	2500	840	1.92
2	PV Cell	0.3	5910	371	406
3	Aluminum (Air duct)	0.3	2719	871	202.4

4.5 Solar Radiation Heat Flux & Ambient Temperature

Solar radiation heat flux and ambient temperature of every hour of the sunny day has been taken for the analysis of cell temperature, power output and efficiency variation with respect to time in the day. Ambient temperature and solar radiation heat flux that strikes on the earth's surface data are as followed [6].

S.NO	Day Time (Hrs)	Ambient Temperature (˚C)	Solar Irradiance Heat Flux (W/m^2)
1	8:00 am	24	300
2	9:00 am	27	500
3	10:00 am	29	625
4	11:00 am	31	700
5	12:00 pm	32	750
6	13:00 pm	33	700
7	14:00 pm	34	600
8	15:00 pm	33	575
9	16:00 pm	32	380
10	17:00 pm	31	200

Above data shows that the solar irradiance remains change with the movement of the sun around the earth. Heat flux will be maximum at peak hours or at azimuth angle and the energy with difference intensity strikes on the upper surface of the PV cell all over the day (in the presence of sun). transmitted or absorbed heat and losses will be required to find out the heat remained in the cell

4.5.1 Heat flux transmitted in the PV Cell

PV Cell doesn't allow all energy into the cell because of material's absorption/transmissivity limitations. As per study carried out, the maximum absorption/transmissivity of the cell is 74% of the total solar irradiance in a day.

$$Htrans = 0.74 \times Hirrad$$

Htrans = Transmitted Heat flux

Hirrad = Solar Irradiance

4.5.2 Radiation Losses

PV module takes out heat to the surrounding environment due to radiations reflection with module. PV module is a non-ideal black body therefore emissivity will be considered for an accuracy of losses.

$$Hrad = \sigma\epsilon \left(T^4_{cell} - T^4_0\right)$$

Hrad = Radiation Losses ($W.m^{-2}$)

σ = Stefan Boltzman constant = $5.678 \times 10^{-8}\ W.m^{-2}.K^{-4}$

ϵ = Emissivity of the surface = 0.88

T_{cell} = Cell temperature (K)

T_0 = Ambient Temperature (K)

4.6 Remaining Heat Flux

Heat remained in the cell is the difference between the heat absorbed by the cell and the radiation losses.

$$Hr = Htrans - Hrad$$

S.NO	Day Time	Ambient Temp:	Solar Irradiance Heat Flux	Solar Rad: Transmitted (Q x0.74)	Radiation Heat Losses	Heat flux Required for Conversion into Power (Q x η)	Heat flux remained in PV Cell
	A	**B**	**C**	**D = C x 0.74**	**E**	**F**	**G = D – E – F – Conv losses**
	Hrs	**˚C**	**W/m^2**	**W/m^2**	**W/m^2**	**W/m^2**	**W/m^2**
1	8:00 am	24	300	222	51.55	30	**140.45**
2	9:00 am	27	500	370	102.10	50	**217.90**
3	10:00 am	29	625	462.5	133.73	62.5	**266.27**
4	11:00 am	31	700	518	159.42	70	**288.58**
5	12:00 pm	32	750	555	160.73	75	**319.27**
6	13:00 pm	33	700	518	162.05	70	**285.95**
7	14:00 pm	34	600	444	147.29	60	**236.71**
8	15:00 pm	33	575	425.5	107.30	57.5	**260.70**
9	16:00 pm	32	380	281.2	69.48	38	**173.72**
10	17:00 pm	31	200	148	40.65	20	**87.35**

4.7 Reynolds Number

Reynold's number is a unitless quantity that is used to define the fluid flow characteristics either flow is laminar or turbulent. It is the ratio of inertia forces to viscous forces.

General equation of reynold's number under follows:

$$Re = \frac{\rho VL}{\mu} = \frac{VL}{\nu}$$

Re = Reynolds Number

ρ= Density

V = Velocity of fluid

L = characteristic length

μ = Dynamic viscosity

ν = Kinematic viscosity

To find the Reynolds number of fluid in a rectangular duct the above equation will be modified as follows:

$$Re = \frac{\rho VDh}{\mu} = \frac{VDh}{\nu} \text{ ..... (1)}$$

D_h = Hydraulic Diameter

$$Dh = \frac{2 \text{ x h x w}}{\text{h} + \text{w}}$$

h = Height of duct (m)

w = width of duct (m)

4.7.1 Reynolds Number of the problem

Hydraulic Diameter:

$$Dh = \frac{2 \text{ x h x w}}{\text{h} + \text{w}} = \frac{2 \text{ x } 0.003 \text{ x } 0.235}{0.003 + 0.235} = 0.00592$$

Put the value of hydraulic diameter equation (1)

$$\boldsymbol{Re} = \frac{5 \text{ x } 0.00592}{1.568 \text{ x } 10\text{e}^{-5}} = \mathbf{1,889}$$

The velocity of the fluid has been taken from data and constant value of kinematic viscosity for air is taken.

5 COMPUTATIONAL FLUID DYNAMICS ANALYSIS

5.1 Introduction

Computational fluid dynamics (CFD) provide a much accurate prediction of fluid flow applications that using mathematical modeling, numerical analysis or software tools to solve the problems. In this problem, CFD softwares are used to simulate the air interaction in the duct attached with the PV Module.

5.2 Methodology

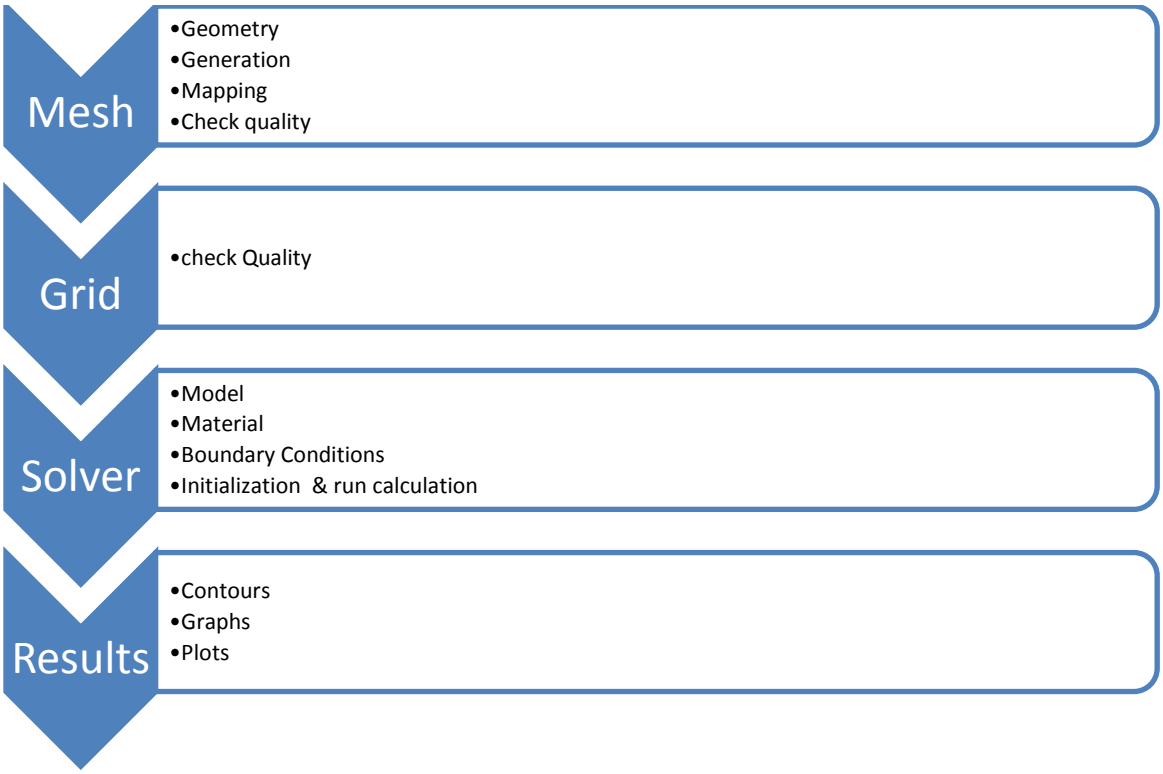

5.2.1 Gambit

Gambit software V 2.4.6 has been used for meshing the required application.

- Geometry
- Mesh generation

- Mesh Quality
- Fluid zone and solid recognizing

5.2.2 ANSYS Fluent

ANSYS Fluent V 15.0 has been used for simulation and solving the problems to get required parameters.

- Grid Check
- Solver
- Model (fluid flow)
- Material specifications
- Boundary conditions
- Initialization
- Case Check
- Run calculations
- Results (contours, graphs & plots)

5.3 Assumptions

- Steady (flow is independent of time)
- Inviscid (flow in which viscosity remains neglected)
- Incompressible (flow in which density remains constant)
- Constant mass flow rate (Inlet = Outlet)
- No heat loss from side walls

5.4 Solar PV Module Mesh

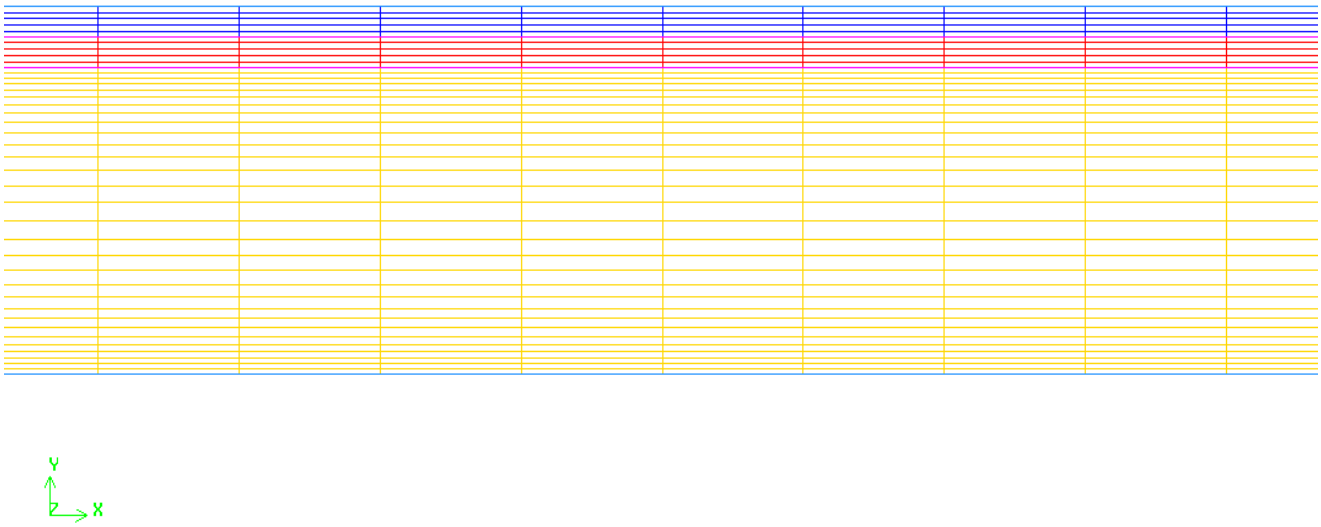

Yellow mesh = Air Duct
Red Mesh = Aluminum Plate
Blue Mesh = Solar PV Cell

5.5 Governing Equations

There are three fundamental laws that can be used to derive governing equations to be solved in CFD study.

- Conservation of mass
- Conservation of linear momentum
- Conservation of energy.

Three dimensional governing equations are made for steady and incompressible flow.

5.5.1 Continuity Equation:

$$\frac{D\rho}{Dt} + \rho(\nabla \cdot \vec{V}) = 0$$

For incompressible flow density has a known constant value. In this study, the flow is steady and incompressible, velocity with respect to time and density will remains constant.

$$\nabla \cdot \vec{V} = 0 \quad \cdots\cdots\cdots\cdots \text{ Eq. A}$$

Or In Cartesian

$$\frac{\partial u}{\partial x} + \frac{\partial v}{\partial y} + \frac{\partial w}{\partial z} = 0$$

Furthermore there is no change in velocity with respect horizontal length (dx). Therefore; continuity equation will become as follows:

$$\frac{\partial v}{\partial y} + \frac{\partial w}{\partial z} = 0$$

It means that the velocity field of an incompressible flow should be divergence free and known as the divergence free constraint. Note that there is no time derivative in the continuity equation

5.5.2 Momentum Equation:

Equation for linear momentum is also known as the Navier-Stokes equation.

$$\rho\left[\frac{\partial \vec{V}}{\partial t} + (\vec{V} \cdot \nabla)\vec{V}\right] = -\nabla p + \mu \nabla^2 \vec{V} + \rho \vec{f}$$

$$\frac{\partial \vec{V}}{\partial t} + (\vec{V} \cdot \nabla)\vec{V} = -\frac{1}{\rho}\nabla p + \nu \nabla^2 \vec{V} + \vec{f}$$

The first term of the equation shows the variation of flow velocity with respect to time. The term $(\vec{V} \cdot \nabla)\vec{V}$ is known as the convective term. It is the term which makes the Navier-Stokes equation nonlinear. $\nu \nabla^2 \vec{V}$ is known as the viscous term or the diffusion term. For steady, incompressible and inviscid flow, the equation will be treated as.

$$\frac{\partial \vec{V}}{\partial t} + (\vec{V} \cdot \nabla)\vec{V} = -\frac{1}{\rho}\nabla p + \nu \nabla^2 \vec{V} + \vec{f}$$

$$(\vec{V} \cdot \nabla)\vec{V} = -\frac{1}{\rho}\nabla p \quad \cdots\cdots\cdots\cdots \text{ Eq. B}$$

Or in Cartesian form.

$$\frac{\partial u_i}{\partial t} + \frac{\partial u_j u_i}{\partial x_j} = \frac{\partial}{\partial x_j}\left(\mu \frac{\partial u_i}{\partial x_j}\right) - \frac{1}{\rho}\frac{\partial p}{\partial x_i}$$

$$\frac{\partial u_j u_i}{\partial x_j} = -\frac{1}{\rho}\frac{\partial p}{\partial x_i}$$

5.5.3 Energy Equation:

Energy equation for incompressible flow can be simplified by considering the fact that density is constant, inviscid flow and $dh = C_p dt$. Therefore energy equation can be written as:

$$\rho c_p \left[\frac{\partial T}{\partial t} + (\vec{V} \cdot \nabla)T\right] = k\nabla^2 T + \phi$$

$$\rho c_p \left[\frac{\partial T}{\partial t} + (\vec{V} \cdot \nabla)T\right] = k\nabla^2 T + \phi$$

$$\boldsymbol{\rho c_p (\vec{V} \cdot \nabla)T = k\nabla^2 T} \quad \text{..... Eq. C}$$

The equation can be written Cartesian form as:

$$\rho c_p \left(\frac{\partial T}{\partial t} + u\frac{\partial T}{\partial x} + v\frac{\partial T}{\partial y} + w\frac{\partial T}{\partial z}\right) = k\left(\frac{\partial^2 T}{\partial x^2} + \frac{\partial^2 T}{\partial y^2} + \frac{\partial^2 T}{\partial z^2}\right) + \phi$$

$$\rho c_p \left(\frac{\partial T}{\partial t} + u\frac{\partial T}{\partial x} + v\frac{\partial T}{\partial y} + w\frac{\partial T}{\partial z}\right) = k\left(\frac{\partial^2 T}{\partial x^2} + \frac{\partial^2 T}{\partial y^2} + \frac{\partial^2 T}{\partial z^2}\right) + \phi$$

Finally it can be written as

$$\rho c_p \left(w\frac{\partial T}{\partial z}\right) = k\left(\frac{\partial^2 T}{\partial y^2} + \frac{\partial^2 T}{\partial z^2}\right)$$

5.6 General Setup

5.6.1 Mesh Scale

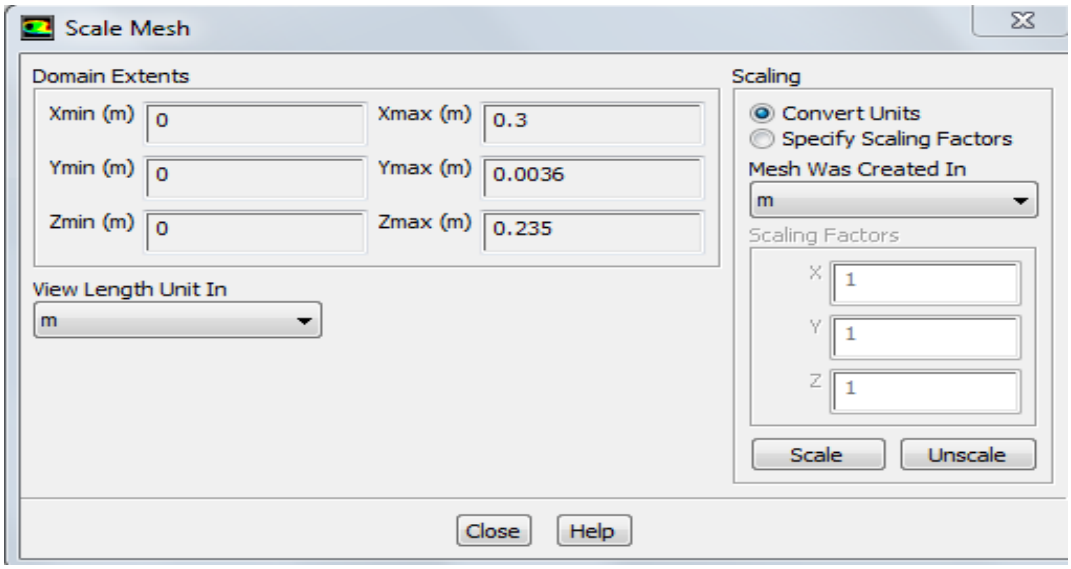

5.6.2 Quality

Orthogonal Quality = 0.997 (Ranges = 0-1 & 0 shows low quality)
Aspect Ratio = 5.90 x $10e^{+1}$

5.6.3 Solver

a. Type:

Pressure based
Density based

The density-based solver solves the governing equations of continuity, momentum, and energy transport and species at the same time (ie, coupled together). On other hand, the solver uses an algorithm based on the pressure, where the equations are solved sequentially (for example, separated from each other). Since the equations are non-linear and coupled. loop solution should be done iteratively to obtain a numerical solution converge.

Pressure based approach has been choose because of low incompressible flow; whereas density based approach is most suitable for high compressible flows. The pressure equation is derived from the continuity and momentum equation in order to correct the velocity field by pressure and to satisfy the continuity [16].

b. Velocity formation:
   - Absolute
   - Relative

The absolute velocity formulation is preferred where the flow in most of the domain is not rotating, whereas relative velocity formulation is most appropriate when fluid is rotating in the domain. For velocity inlets and walls, velocity may specify either the absolute or the relative frame [16].

c. Time:

   - Steady
   - Transient

Flow in which all parameters (pressure, velocity or other) do not depends on time is called steady and flow which is dependent on time is called transient or unsteady. In this study, flow is assumed to be steady. There will be no change in velocity at any point with respect to time and the fluid remains steady across the domain (duct).

5.7 Model & Material

Energy – On
Viscous – Laminar
Radiation – Off
Heat Exchanger – Off
Solidification & Melting – Off
Eulerian Wall Film – Off

Energy equation has been used to set all parameters regarding energy and heat transfer. Flow is taken as laminar because calculated Reynolds numbers are less than 2,300. Laminar is generally happens when dealing small ducts or low flow velocity. All other modeling are not related or not to be assumed in this study.

S.No	Material	Density **Kg/m^3**	Sp. Heat **j/kgK**	Thermal conductivity **w/mK**
1	Air (Fluid)	1.225	1006.43	0.0242
2	PV Cell (Solid)	5910	371	406
3	Aluminum (Solid)	2719	871	202.4

5.8 Boundary Conditions

- Inlet = Mass Flow Inlet
- Outlet = Outflow
- Side walls = Adiabatic (no heat loss or gain)

It is assumed that the mass flow inlet and outlet will be the same across the duct. Therefore outflow has been taken at outlet.

5.9 Solution Methods

5.9.1 Pressure-Velocity Coupling

- SIMPLE (Semi Implicit Method for Pressure Linked Equation)
- SIMPLEC (Semi Implicit Method for Pressure Linked Equation Consistent)
- Coupled
- PISO (Pressure Implicit with Splitting Operations)

SIMPLE algorithm is the numerical procedure used mainly to solve the NS equation SIMPLE algorithm uses the relationship between velocity and pressure corrections to enforce the conservation of mass and for the pressure field. The **SIMPLEC** procedure is similar to the SIMPLE procedure and the only difference lies in the expression used for the face flux correction. The steps involved are same as the SIMPLE algorithm and the algorithm is iterative in nature. **PISO** is an extension of the SIMPLE algorithm used in CFD computational fluid dynamics to solve the Navier-Stokes equations. PISO is a pressure-velocity calculation procedure for the Navier-Stokes equations developed originally for non-iterative computation of unsteady compressible flow, but it has been adapted successfully to steady-state problems [14].

Coupled approach has been chosen from above options because of the coupled approach offers some advantages over the non-coupled or segregated approach. The coupled scheme obtains a robust and efficient single phase implementation for steady-state flows, with superior performance compared to segregated solution schemes [16]. The algorithm based on the pressure segregation solves the equation of momentum and pressure correction subsequently. This semi-implicit solution method results in slow convergence.

5.9.2 Spatial Discritization

Gradient:

- Green-Gauss Cell Based
- Green-Gauss Node Based
- Least Square Cell Based

Gradients are not only required to build the scalar values in the faces of cells, but also for the calculation of the diffusion term and derivatives of velocity. Gradients are used for the sampling of convective and diffusive terms in the conservation equations flow. ANSYS Fluent degraded calculated according to the following above methods [16].

Green-Gauss Cell Based is least computationally intensive and solution may have false diffusion. **Green-Gauss Node Based** is more accurate intensive, minimize false diffusion and it is recommended for unstructured mesh. **Least Square Cell Based** is having the same accurateness and properties as Node Based Gradient and it is less computationally intensive.

Least square cell based gradient has been taken suitable for the solution. least squares gradients based cells are available for use and its accuracy is comparable to the node gradients based, it is better than the node based gradients used in these screens, as they are known to be more stable [16].

ANSYS Fluent allows to choose the discretization scheme for the convection terms of each governing equation. Single-phase problems using either the pressure-based or density-based solver are solved using second-order upwind discretization for the convection terms of the flow equations and all scalar equations except those for turbulence quantities, which are solved using

first-order upwind discretization. For multiphase flows, the flow equations use first-order upwind discretization by default [16].

Pressure:

- Standard
- Second order
- PRESTO
- Linear
- Body forced weighted

Standard scheme interpolates the pressure on the faces using the cell center values. Accuracy reduced for flows exhibiting large surface-normal pressure gradients near boundaries. On the other hand **PRESTO** discretization for pressure actually calculates pressure on the face. PRESTO discretization gives more accurate results as interpolation errors and pressure gradient assumptions on boundaries are avoided. It use for highly swirling flows, flows involving steep pressure gradients (porous media, fan model, etc.), or in strongly curved domains. **Linear** scheme use when other options result in convergence face difficulties. Body Force Weighted involves in large body forces (i.e. high swirling flows).

Second-Order is mostly used for compressible flows and cannot be used for with porous, fan or multiphase flow. It can also be used for accuracy when other schemes are not applicable. **Second order** discretization is recommended more accurate from the following above options.

Momentum & Energy:

- First Order Upwind
- Second Order Upwind
- Power Law
- QUICK
- Third Order MUSCL

In **First Order Upwind** quantities at cell faces are determined by assuming that the cell-center values of any field variable represent a cell-average value and keep throughout the entire cell; the

face quantities are the same to the cell quantities. It is known as the more accurate and easy to converge. The **Power-Law** discretization scheme interpolates the face value of a variable and it is more accurate than first order upwind for flows having low Reynolds number. **Second Order Upwind** quantities at cell faces are computed using a multidimensional linear reconstruction approach. In this approach, higher-order accuracy is achieved at cell faces through a Taylor series expansion of the cell-centered solution about the cell centroid. **QUICK** scheme computes a higher order value of the convected variable ϕ at a face for quadrilateral and hexahedral meshes, where unique upstream and downstream faces. It is also useful for swirling flows. **MUSCL** (Monotonic Upstream-Centered Scheme for Conservation Laws) 3rd order convection discretisation scheme for unstructured meshes; more accurate in predicting secondary flows, vortices, forces, etc

Second Order Upwind discretization is recommended as more accurate from the following above options

5.10 Solution Controls

Pseudo Transient Explicit Relaxation Factors:
Pressure = 0.3
Momentum = 0.3
Density = 1
Body Forces = 1
Energy = 0.75

5.11 Initialization

Full Multigrid (FMG) initialization method has been utilized for better and accurate solution. It is used for steady, laminar and single phase flow. Mostly FMG used for complex flow problems just like flow in rotating machinery and spiral duct. FMG can provide initial and approximate solution at a minimum cost to the overall computational cost [16].

The overall initialization time using this approach is much longer than that using standard initialization by zone, but it allows a much quicker solve. FMG solves euler equations and is available for single-phase flows only [16].

Command:

>Solve/initialization/

>Solve/initialization/fmg

FMG Limits: it will not be used for unsteady, turbulent and multiphase flows.

5.12 Convergence

All cases have been converged around 4000 iterations. Convergence figure of all cases is attached in Annex-I

6 RESULTS AND DISCUSSION

6.1 Temperature, Velocity & Pressure (PVT) Profiles

The total height (thickness) of the flow duct is 3mm and the length and width of the cross-section is 300mm and 235mm respectively. Graphs of these properties has been taken on different heights of the duct near to the under observation cell surface (cell surface is at 3mm height), such as at 1.5mm (centre), 2.00mm & 2.5mm respectively.

6.2 Temperature Profile

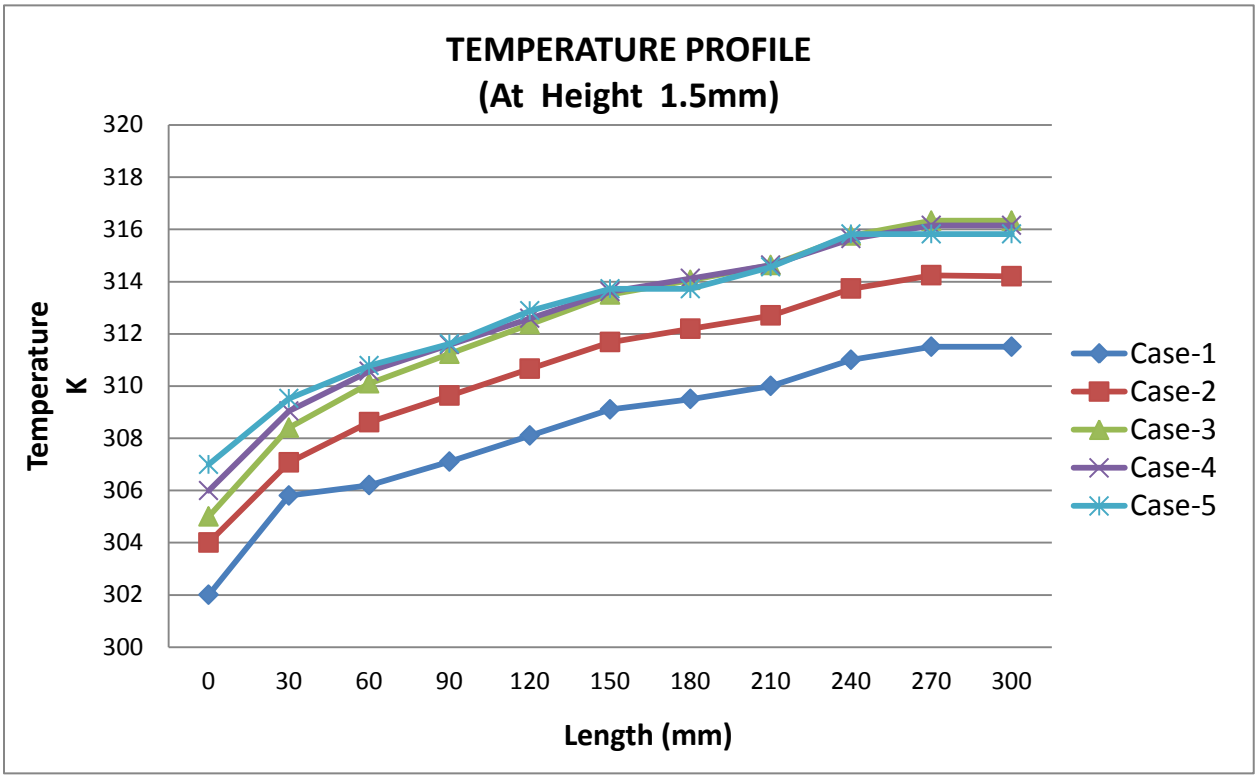

Graph 6–1 : Temperature profile of fluid at 1.5mm height (centre)

The x-axis on this graph shows the total length of the simulated cell while temperature variation in fluid (air) with respect to the length appears on y-axis. 0mm origin is the flow inlet point and 300mm is outlet point respectively.

In each case, temperature of the air increases proportionally with the distance covered by air. Air that flows through the duct in contact with cell surface carries out remaining heat from the duct

and heat transfers from the cell into air that increases air temperature gradually like as heat exchanger process (heat flows from high temperature to low temperature).

The temperature variation in air flow at height 2.0 and 2.5mm having the same pattern in the flowing duct as at the height of 1.5mm which are followed below.

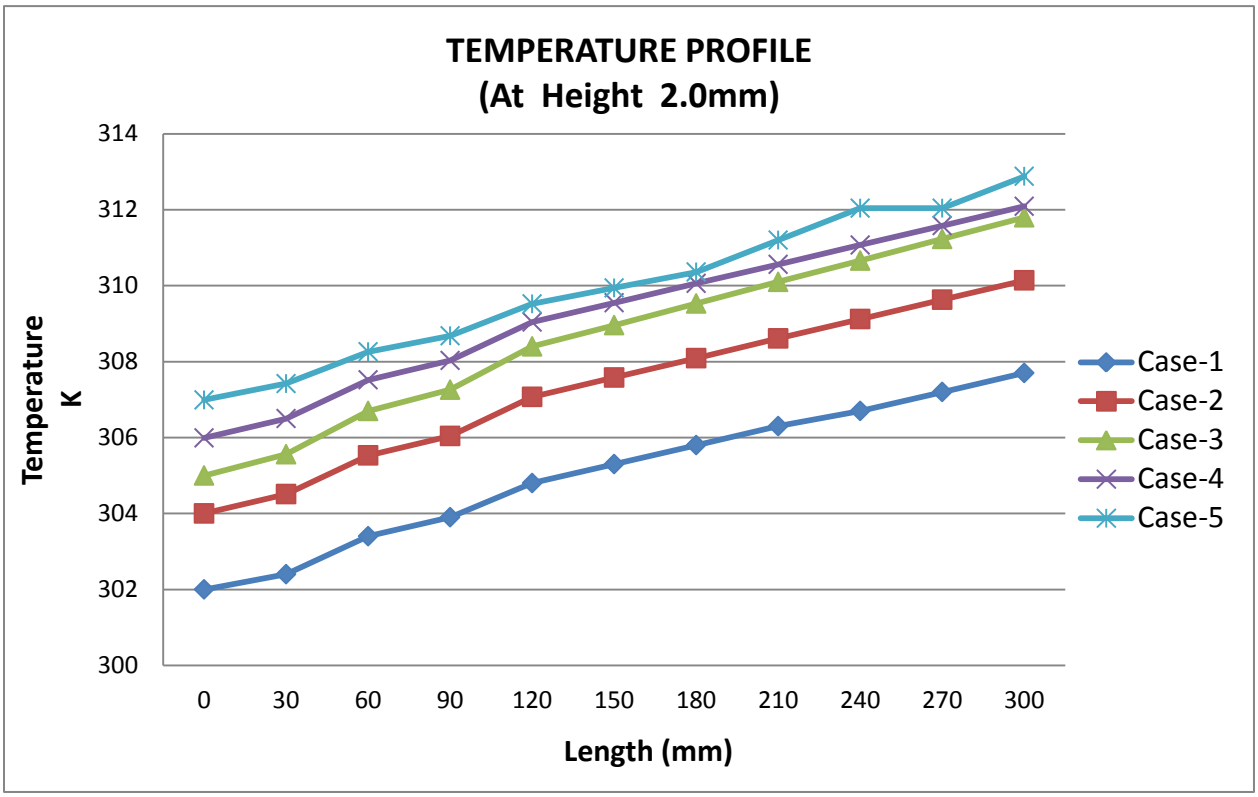

Graph 6–2 : Temperature profile of fluid at 2.0mm height

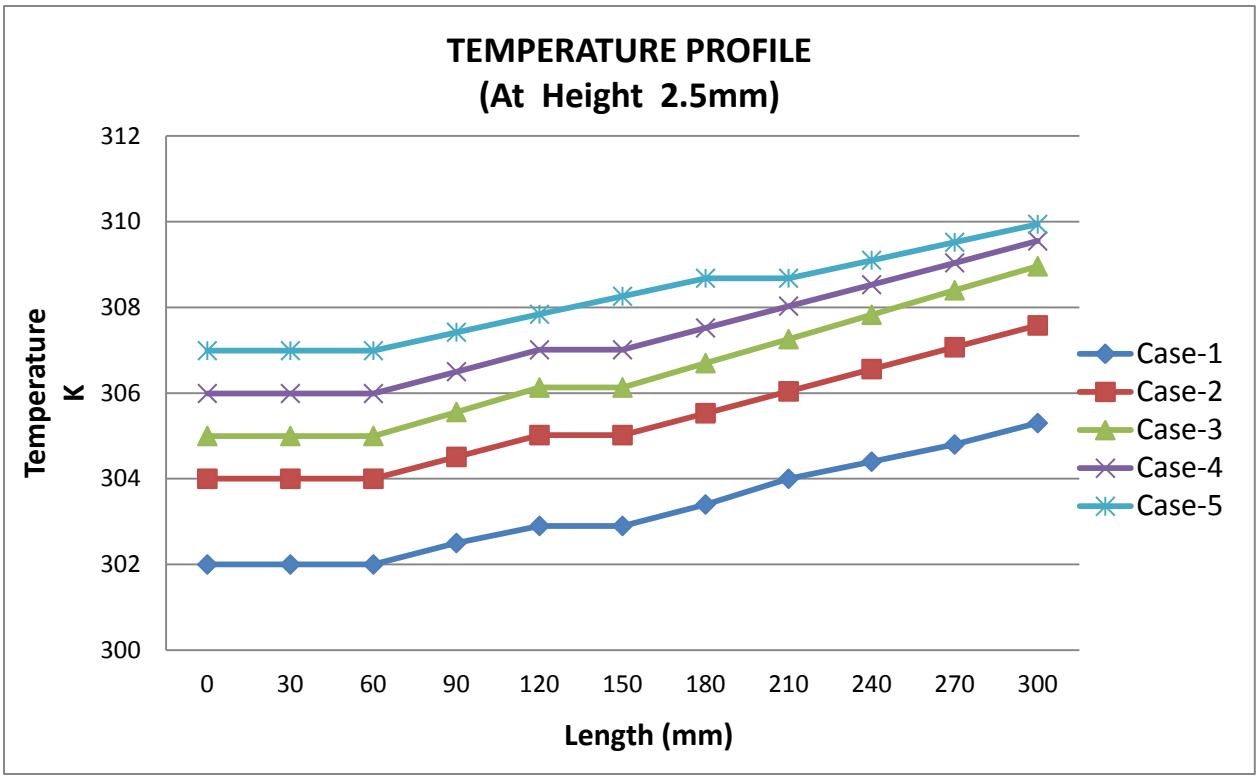

Graph 6–3 : Temperature profile of fluid at 2.5mm height

6.3 Velocity Profiles

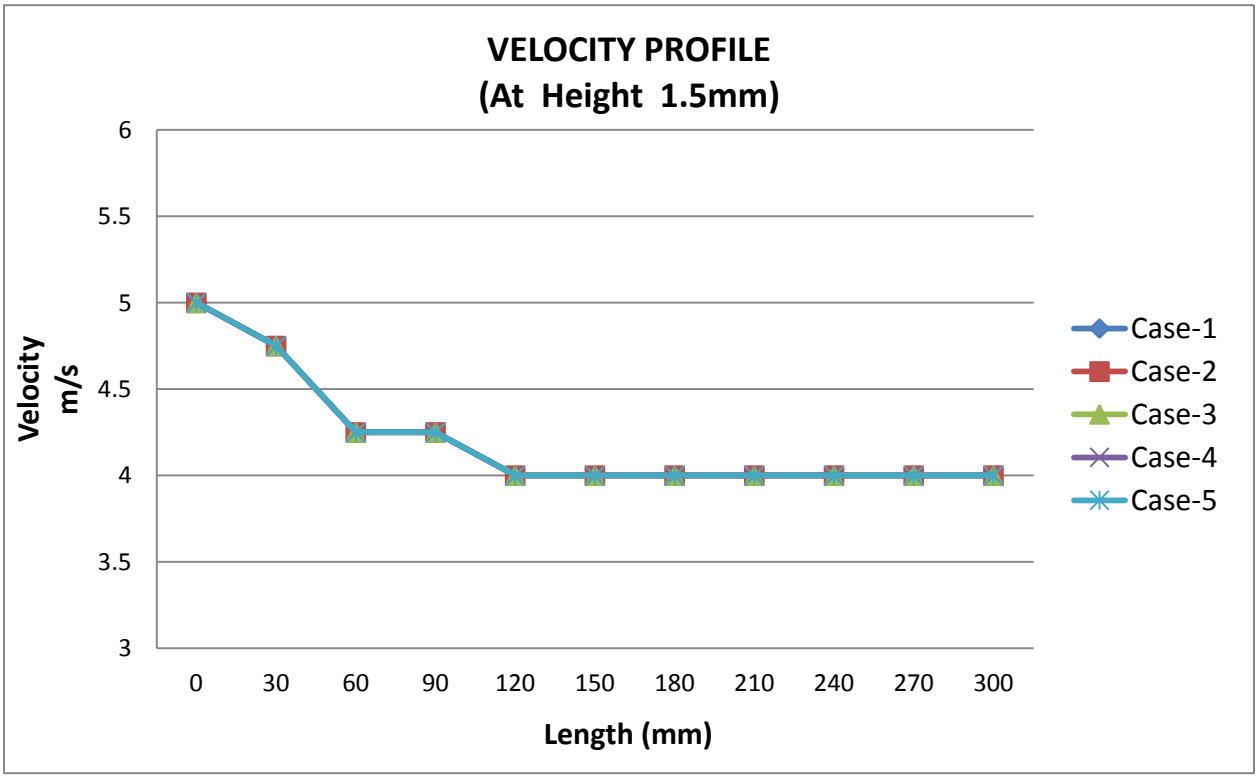

Graph 6–4 : Velocity profile of fluid at 1.5mm height (centre)

The x-axis on this graph shows the total length of the simulated cell and velocity variation in fluid (air) with respect to length appears on y-axis. 0mm origin is the flow inlet point and 300mm is outlet point respectively.

In each case, Velocity of the fluid drops down gradually in the starting of the cell. When air reached at the centre of the cell, the velocity of the cell remains stable.

The velocity variation in air flow at height 2.0 and 2.5mm having the same pattern in the flowing duct as at the height of 1.5mm which are followed below.

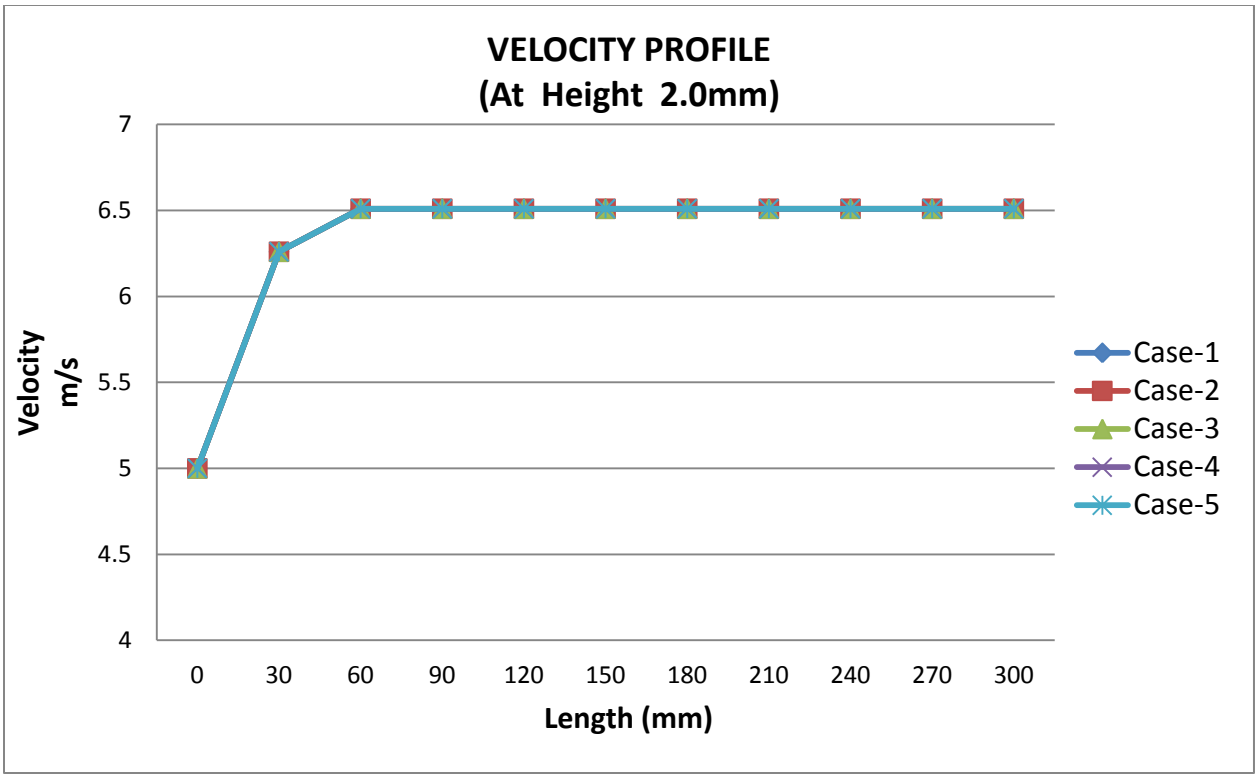

Graph 6–5 : Velocity profile of fluid at 2.0mm height

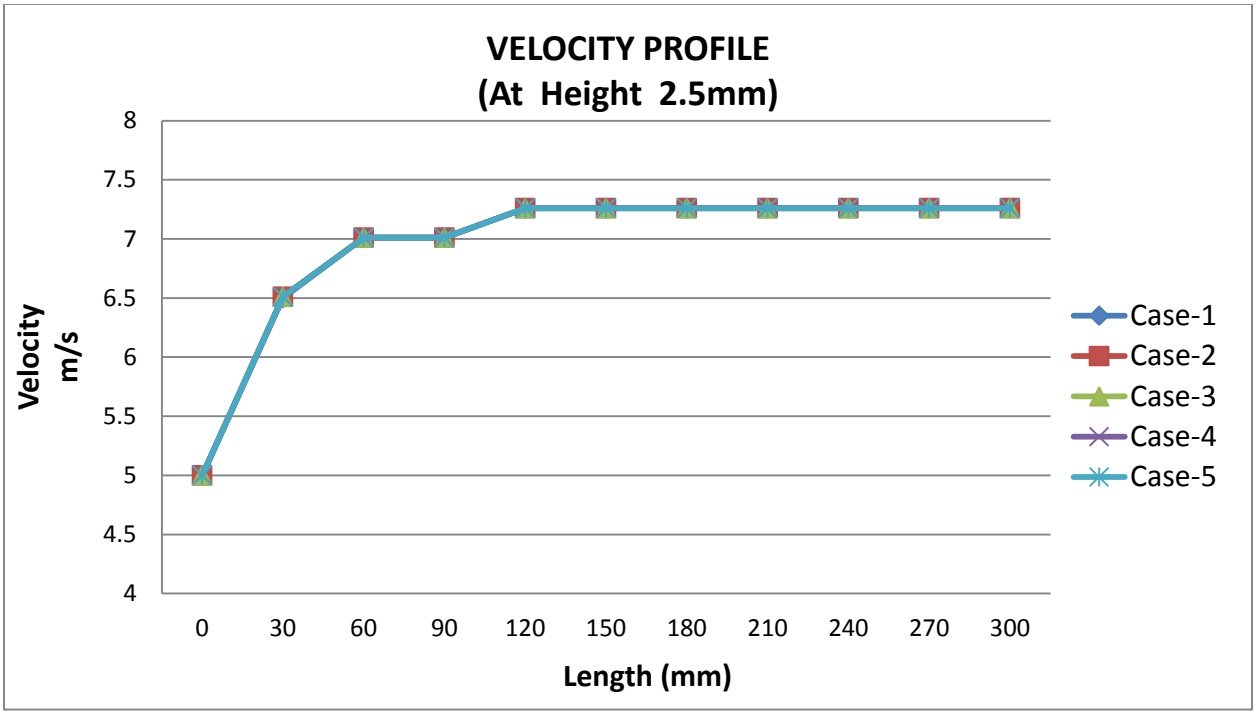

Graph 6–6 : Velocity profile of fluid at 2.5mm height

6.4 Pressure Profiles

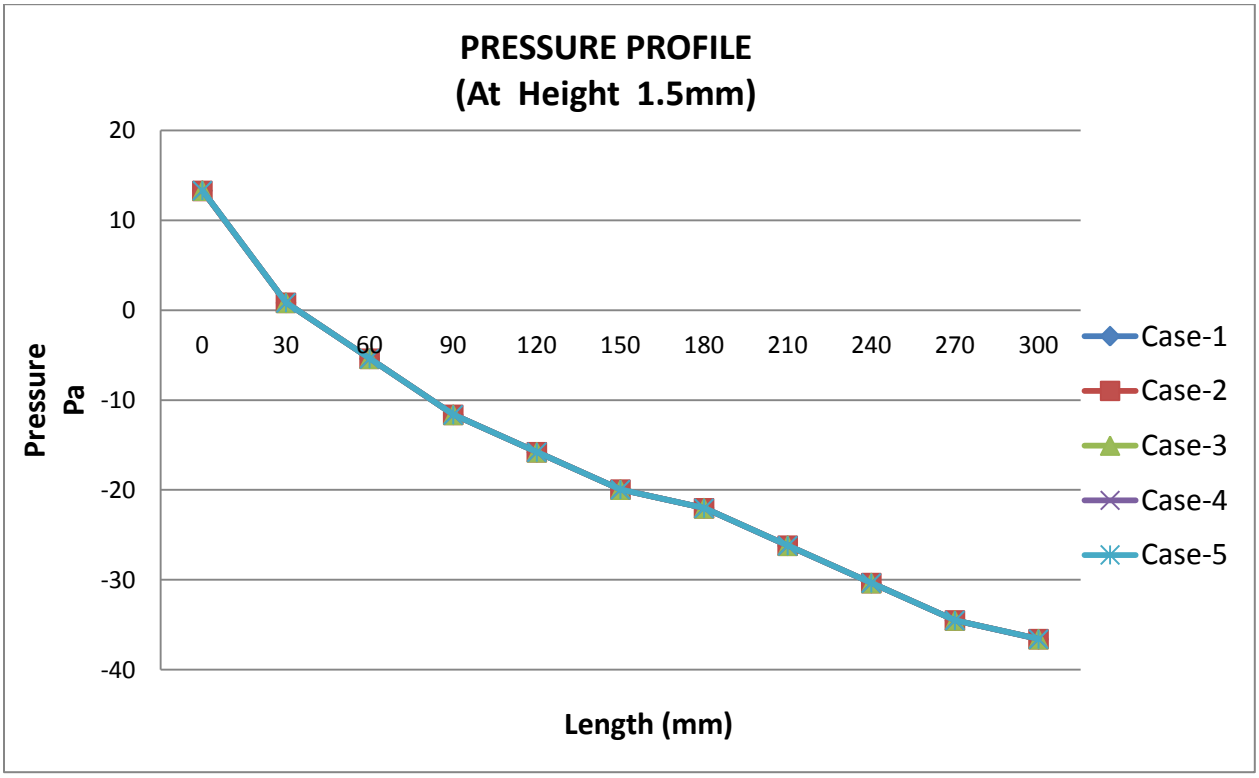

Graph 6–7 : Pressure profile of fluid at 1.5mm height (center)

The x-axis on this graph shows the total length of the simulated cell and pressure variation in fluid (air) appears on y-axis. 0mm origin is the flow inlet point and 300mm is outlet point respectively.

All pressure graphs show that pressure gradually drops down with respect to the distance covered by flow from inlet till outlet. According to principle of wind energy (air motion), the air always flow from high pressure to low pressure and drop in pressure occurs due to gradually increase of heat in flow.

At all three heights in the duct at the same point (length), the pressure near to the surface (cell) becomes slightly higher than the pressure away from the surface. This happens because of high temperature at the cell and lower temperature in the air. As we know temperature is directly proportional to the pressure.

The pressure variation in air flow at height 2.0 and 2.5mm having the same pattern in the flowing duct as at the height of 1.5mm which are followed below.

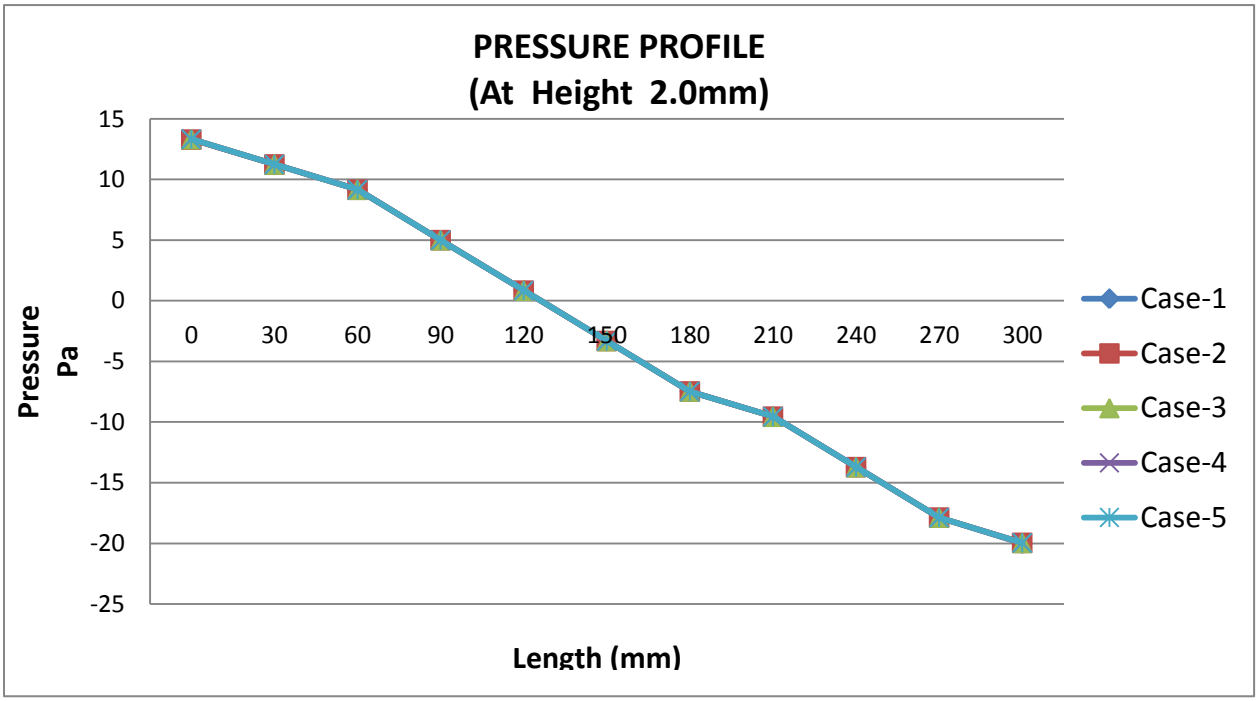

Graph 6–8 : Pressure profile of fluid at 2.0mm height

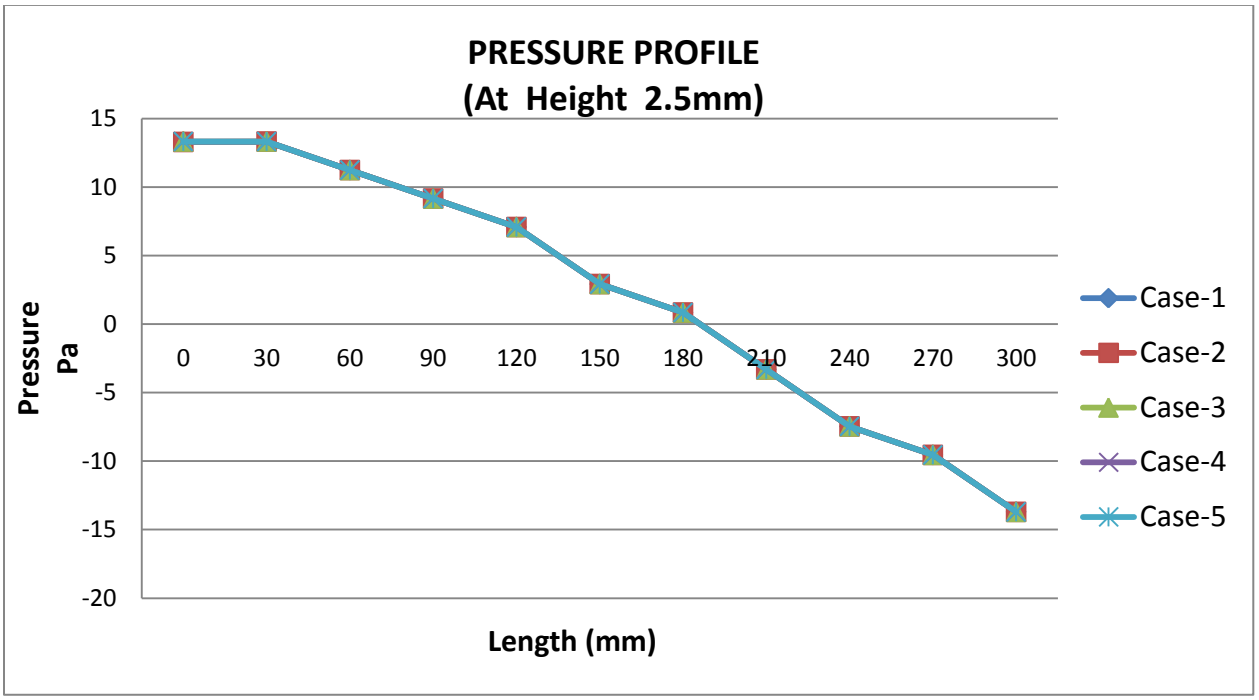

Graph 6–9 : Pressure profile of fluid at 2.5mm height

6.5 Cell Temperature

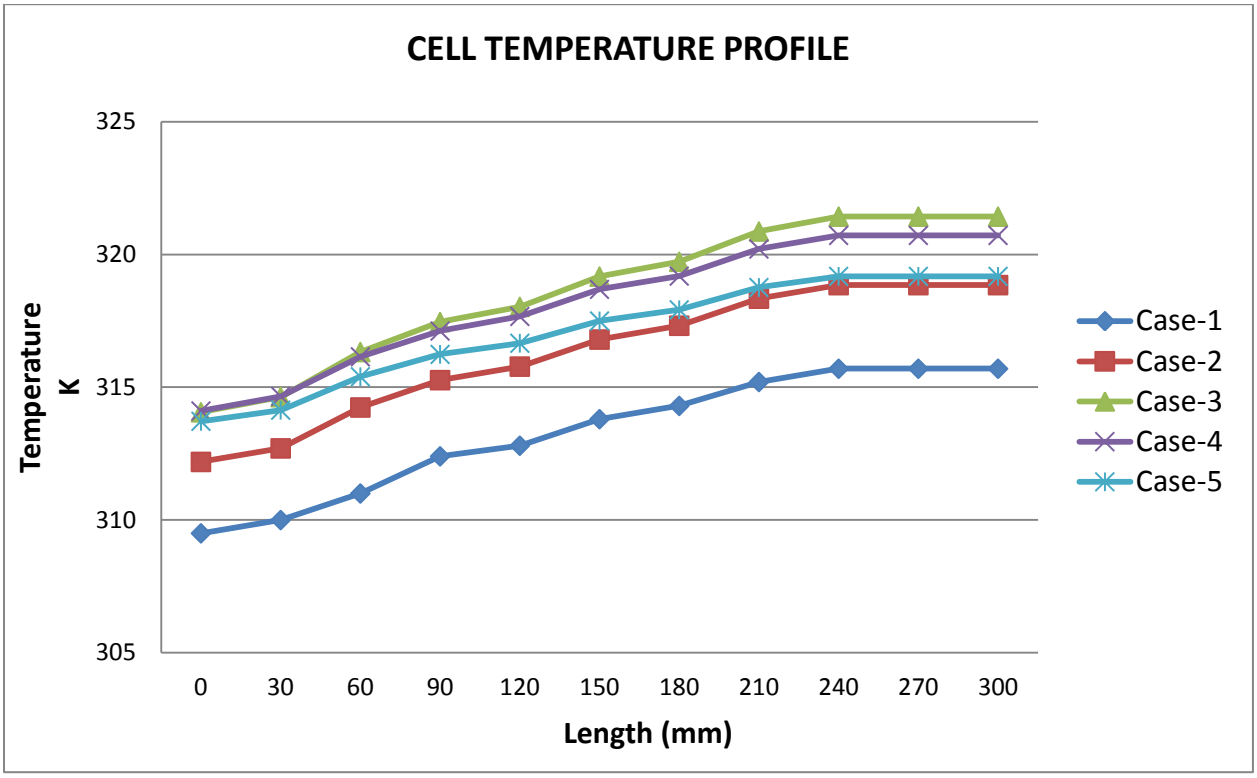

Graph 6–10 : Cell temperature profile

Above profile shows the variation of cell temperature with respect to the length of the duct. Air (fluid) injected from the 0mm length towards 300mm outlet and it shows that cell temperature increases because of increase in air temperature. In the beginning air temperature at 302k decreases the actual cell temperature effectively but with respect to transient the air from the duct causes gradually increase in the temperature of the air because of heat transfer from cell surface. Therefore the temperature difference outline between the air and cell will be the same at any point of the duct. Cell temperature figures of all cases are attached in **Annex-II**.

6.6 Power & Efficiency Graphs

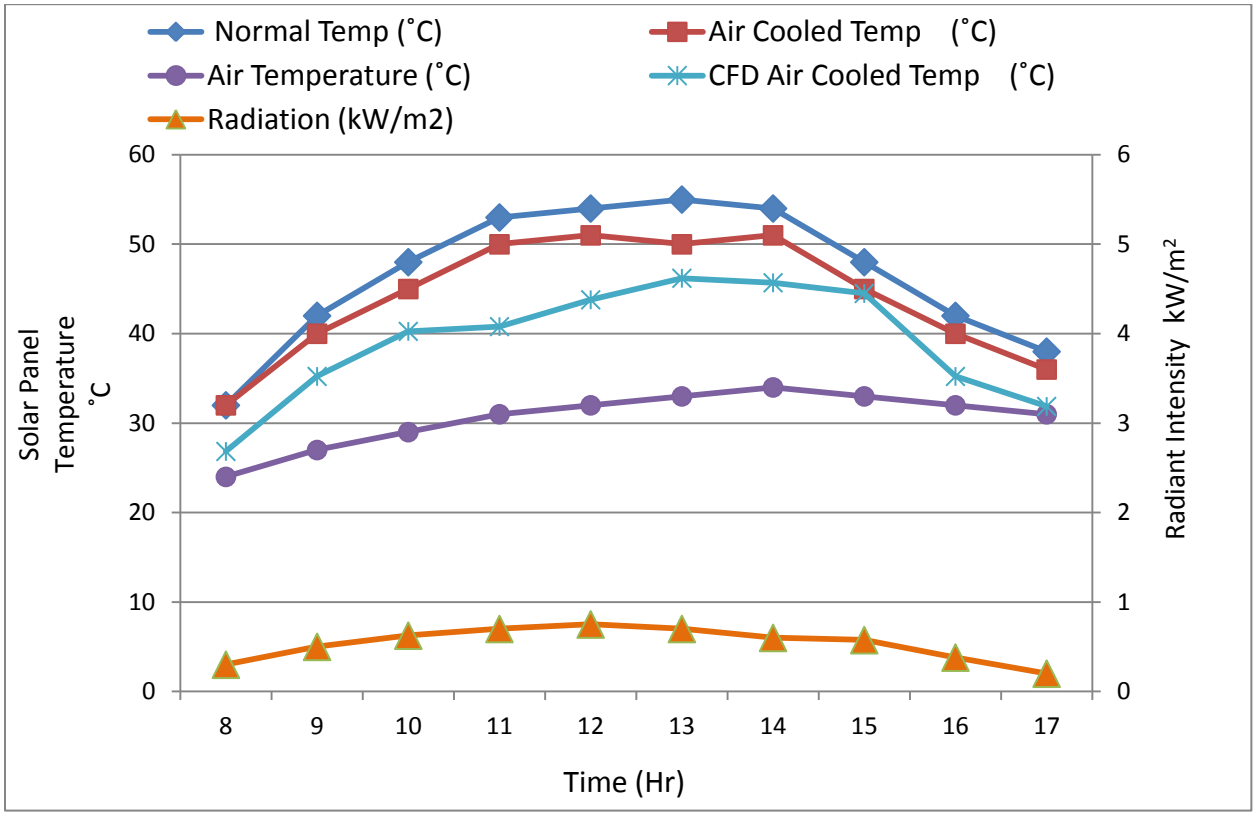

Graph 6–11 : Cell Temperature of the PV Cells

Above graph shows the radiation and temperature differences in the day time hours, including solar radiation in kW/m^2, Air Temperature (ambient air temperature), Normal temperature (conventional PV cell temperature), air cooled temperature (reference research cell temperature) and CFD air cooled temperature (CFD modified PV cell temperature). All parameters are proportional to each other.

The x-axis on this graph shows the day time hours from 08:00am to 17:00pm and temperature (˚C) variation of the cell appears on primary y-axis (left) and radiation (kW/m^2) appears on secondary y-axis.

The maximum radiation intensity is 750W/m^2, whereas the maximum normal, air cooled and CFD modified cell temperature are 55˚C, 51˚C & 46˚C respectively. The minimum and maximum temperature difference between normal and CFD modified PV cell temperature is

3.2˚C and 12.2˚C. The affects of cell temperature on power and efficiency are mentioned in the below graphs.

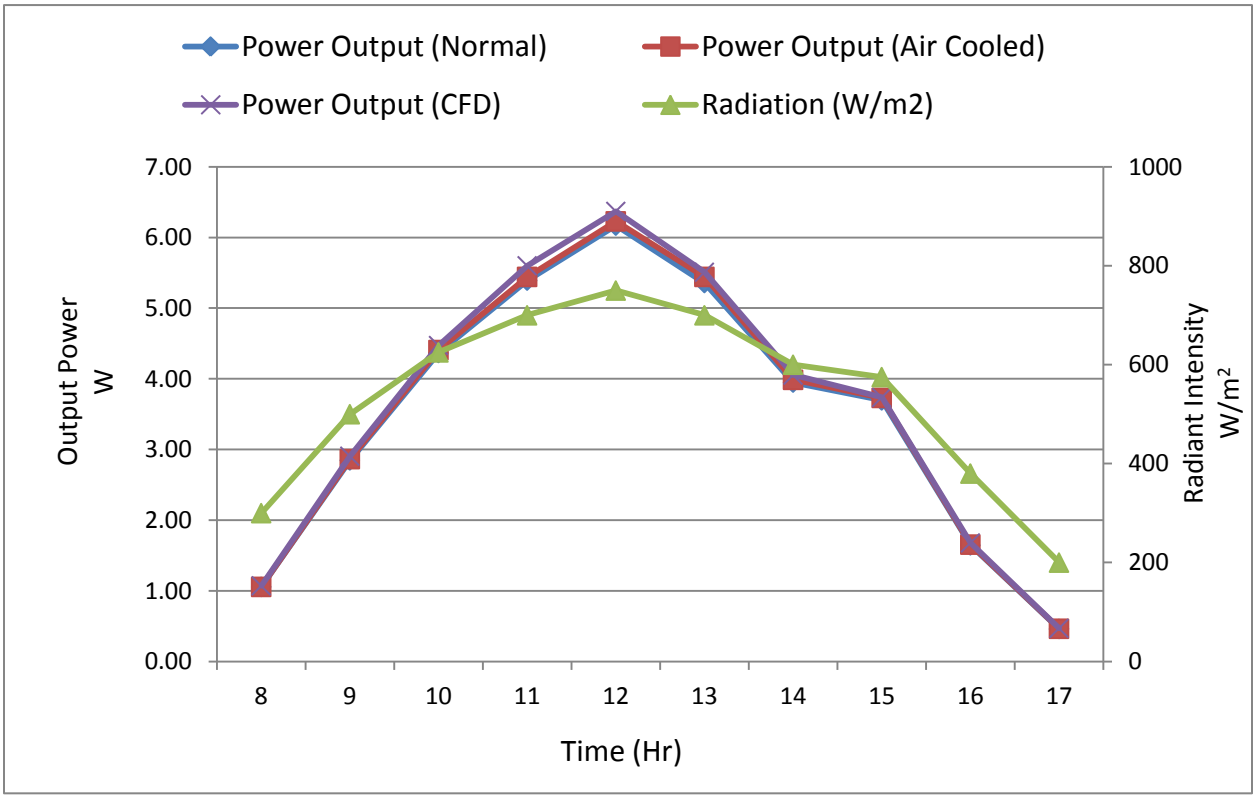

Graph 6–12 : Power output of the PV Cells

Above graph shows the radiation and temperature differences in the day time hours, including solar radiation (W/m^2), normal power output (conventional PV power), air cooled PV power output (reference research cell power) and CFD air cooled power output (CFD modified PV cell).

The x-axis on this graph shows the day time hours from 08:00am to 17:00pm and power outputs (W) of the cell appears on primary y-axis (left) and radiation (W/m^2) appears on secondary y-axis.

The maximum radiation intensity is 750W/m^2, the maximum normal, air cooled and CFD modified cell power outs are 6.17W, 6.23W & 6.35W respectively. The minimum and maximum power output difference between normal and CFD modified PV cell is 0.04W and 0.21W.

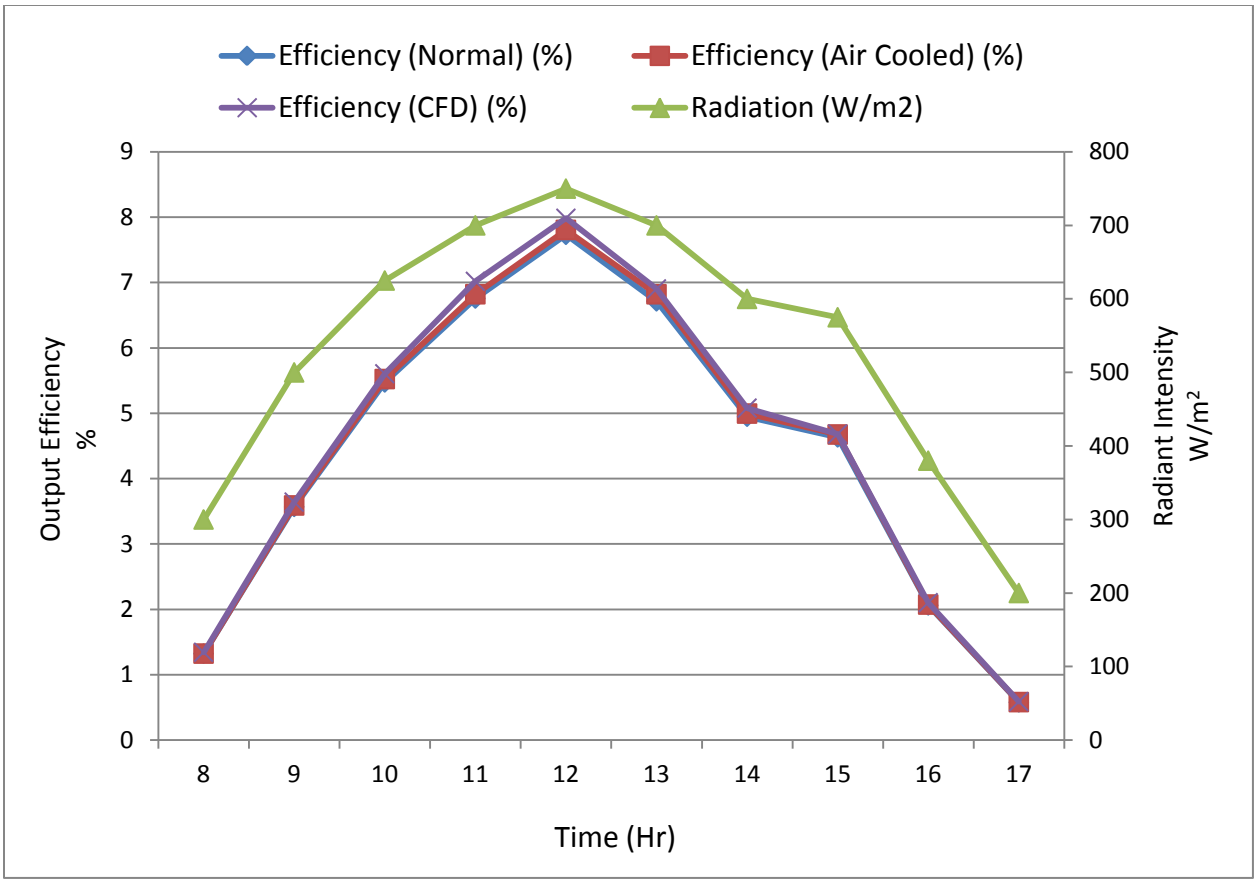

Graph 6–13 : Efficiency of the PV Cells

Above graph shows the radiation and temperature differences in the day time hours, including solar radiation (W/m^2), normal cell efficiency (conventional PV power), air cooled PV cell efficiency (reference research cell power) and CFD air cooled cell efficiency (CFD modified PV cell).

The x-axis on this graph shows the day time hours from 08:00am to 17:00pm and effiency of the cells appears on primary y-axis (left) and radiation (W/m^2) appears on secondary y-axis.

The maximum radiation intensity is $750W/m^2$, the maximum normal, air cooled and CFD modified cell power outs are 7.73%, 7.81% & 7.98% respectively. Otherwise the rated efficiency of the cell is 10%. The minimum and maximum power output difference between normal and CFD modified PV cell is 0.1% and 0.25%.

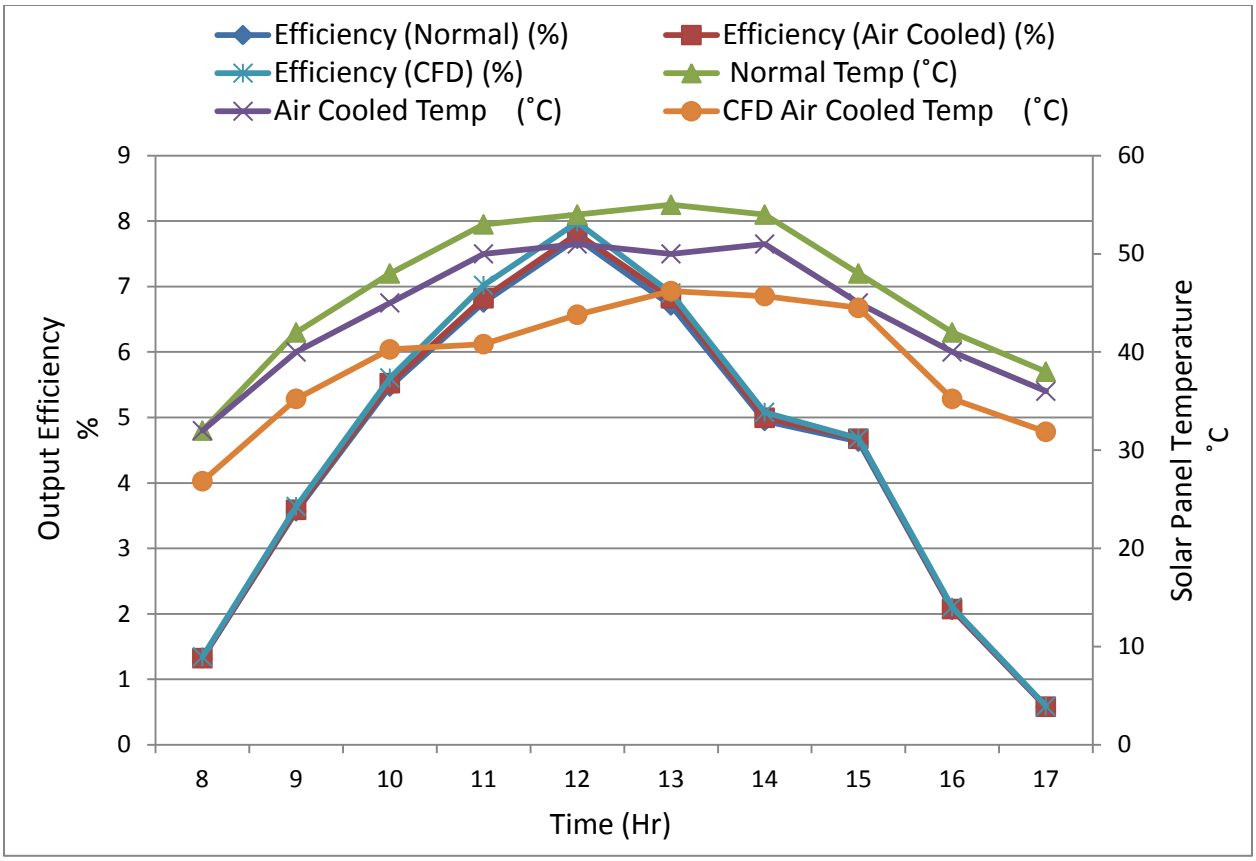

Graph 6–14 : Cell Temperature & Efficiency of the PV Cells

Above graph shows the radiation, temperature and efficiency differences in the day time hours, including normal cell efficiency (conventional PV power), air cooled PV cell efficiency (reference research cell power), CFD air cooled cell efficiency (CFD modified PV cell), Normal temperature (conventional PV cell temperature), air cooled temperature (reference research cell temperature) and CFD air cooled temperature (CFD modified PV cell temperature).

The x-axis on this graph shows the day time hours from 08:00am to 17:00pm and efficiency of the cells appears on primary y-axis (left) and temperature (˚C) appears on secondary y-axis.

The maximum normal, air cooled and CFD modified cell power outs are 7.73%, 7.81% & 7.98%. While the maximum normal, air cooled and CFD modified cell temperature are 55˚C, 51˚C & 46˚C respectively. Following results shows that the decrease in cell temperature caused proportionally increase in the power and efficiency of the cell.

7 CONCLUSION

The Study of ""**"Computational Fluid Dynamics Analysis and Modification of Solar Photovoltaic Modules"** has been carried out to improvise the drawbacks of most utilized alternative energy technology. This study narrates the effects of external environmental parameters on efficiency of the PV module along with the identification of sensitive layer (cell) temperature effects on power & efficiency of the module. PV module has been remodified by using CFD Simulation softwares in order to reduce the cell temperature.

Micro plate air duct made of aluminum have been introduced at the back of the cell to modify conventional solar PV module and also ensure that the heat pipe contact closely enough to cell, at last thermal insulation used to reduce energy losses.

Heat in the cell dissipated away from the PV cell through the air duct, uninterrupted supply of air through duct reduces the temperature of the cell that in result increases the PV conversion efficiency. Differences in results of modified solar PV module with conventional Solar Module were further discussed in this study

Required results were achieved in CFD simulations and the relation of cell temperature with power and efficiency of the cell have been emphasized in this study. The maximum temperature, power and efficiency difference between the normal and CFD modified PV cell were achieved upto 12˚C, 0.21W and 0.21%. Cell temperature, power and efficiency data of all cases is can be seen in **Annex III**.

It is concluded by results that the 3% to 5% of the total power can be increased by using modified technology. The motivation of this study is to utilize alternative energy technologies in an efficient manner to enhance green environment and to reduce financial cost.

REFERENCE

[1] www.pres.org.pk/category/reaepakistan/re-scenario

[2] Batoul, H. "Flow Simulation improves Photovoltaic Solar Panel Performance", Technical director of solar Department, Schueco International, Paris, France

[3] Hughes, B.R., Cherisa, N.P.G and Beg, O., "Computational study of improving the efficiency of Photovoltaic Panels in the UAE"

[4] Krauter, S., "Increased electrical yield via water flow over the front of Photovoltaic Panels", Department of physics, federal state university of Ceara, Brazile.

[5] "PV/T Solar Duct" Conserval Engineering Inc, 200 Wildcat Rd. Toronto, Canada, www.solarwall.com

[6] Tang, X., Quan, Z. and Zhao, Y., "Experimental Investigation of Solar Panel Cooling by a Novel Micro Heat Pipe Array", Architectural and Civil Engineering Institute, Beijing University of Technology, Beijing, China.

[7] Subarkah, R. and Belyamin, "Improved Efficiency Solar Cells with Forced Cooling Water", Jurusan Teknik Mesin, Politeknik Negeri Jakarta, DEPOK, Indonesia.

[8] Zhu, L., Boehm, R.F., Wang, Y., Halford, C. and Sun, Y., "Water immersion cooling of PV cells in a high concentration system", Center for Energy Research, University of Nevada, Las vegas, USA, August 2010.

[9] Barsegyan, H., "What is the Effect of Temperature on Solar Cells?", California State Science Fair, 2006 Project Summary.

[10] "Theory of solar cells", www.wikipedia.com, (http://en.wikipedia.org/wiki/Theory_of_solar_cells#Cell_temperature)

[11] Cozzini, M., “solar cell cooling and heat recovery in a concentrated photovoltaic system”, Renewable Energies and Environmental Technologies (REET) unit, Trento, Italy.

[12] Fontenault[1], B.J. and Gutierrez-Miravete[2], E., “Modeling a Combined Photovoltaic-Thermal Solar Panel”, General Dynamic Electric Boat Corporation[1] and Rensselair Polytechnic Institute[2], Windsor Street, Hartford.

[13] Teo, H.G., Lee,P.S., and Hawlader, M.N.A., “An active cooling system for photovoltaic module”, National University of Singapore, Singapore.

[14] www.wikipedia.com

[15] www.pveducation.org

[16] Fluent User’s Guide

ANNEX-I

CONVERGENCE

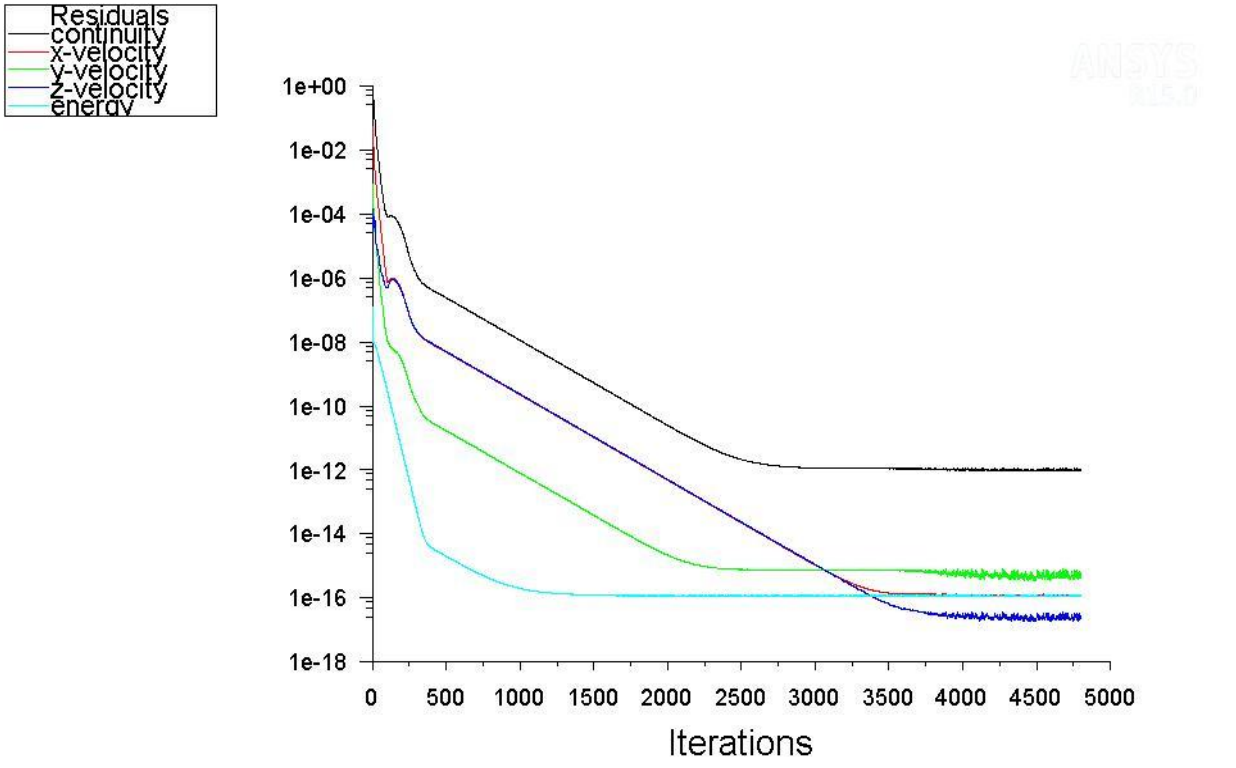

Case-1:

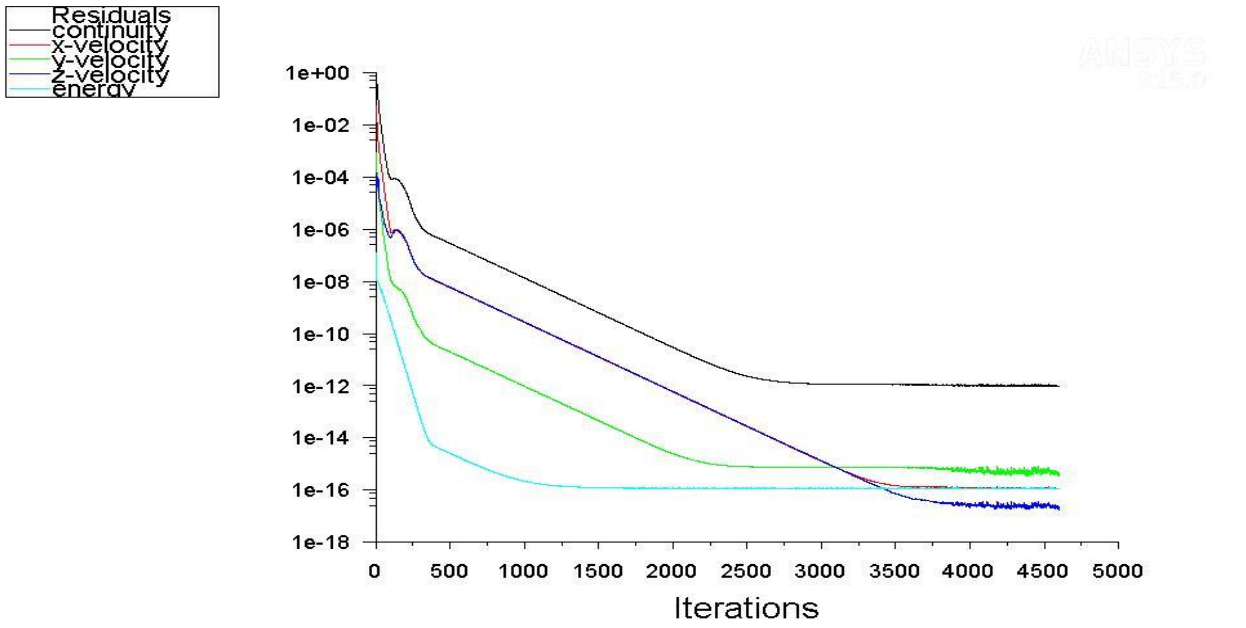
Residuals
continuity
x-velocity
y-velocity
z-velocity
energy
1e+00
1e-02
1e-04
1e-06
1e-08
1e-10
1e-12
1e-14
1e-16
1e-18
0
500
1000
1500
2000
2500
3000
3500
4000
4500
5000
Iterations
Scaled Residuals
Jun 07, 2015
ANSYS Fluent 15.0 (3d, dp, pbns, lam)

Case-2

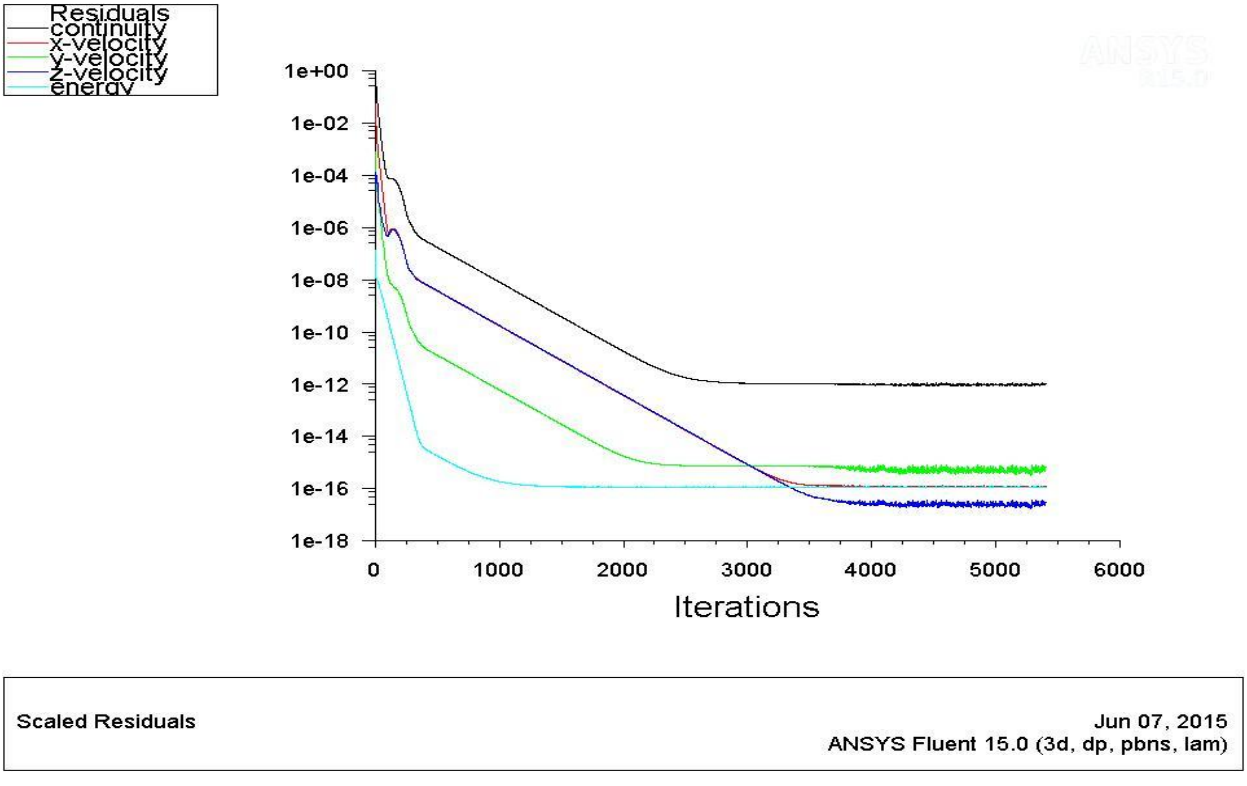
Residuals
continuity
x-velocity
y-velocity
z-velocity
energy
1e+00
1e-02
1e-04
1e-06
1e-08
1e-10
1e-12
1e-14
1e-16
1e-18
0
1000
2000
3000
4000
5000
6000
Iterations
Scaled Residuals
Jun 07, 2015
ANSYS Fluent 15.0 (3d, dp, pbns, lam)

Case-3

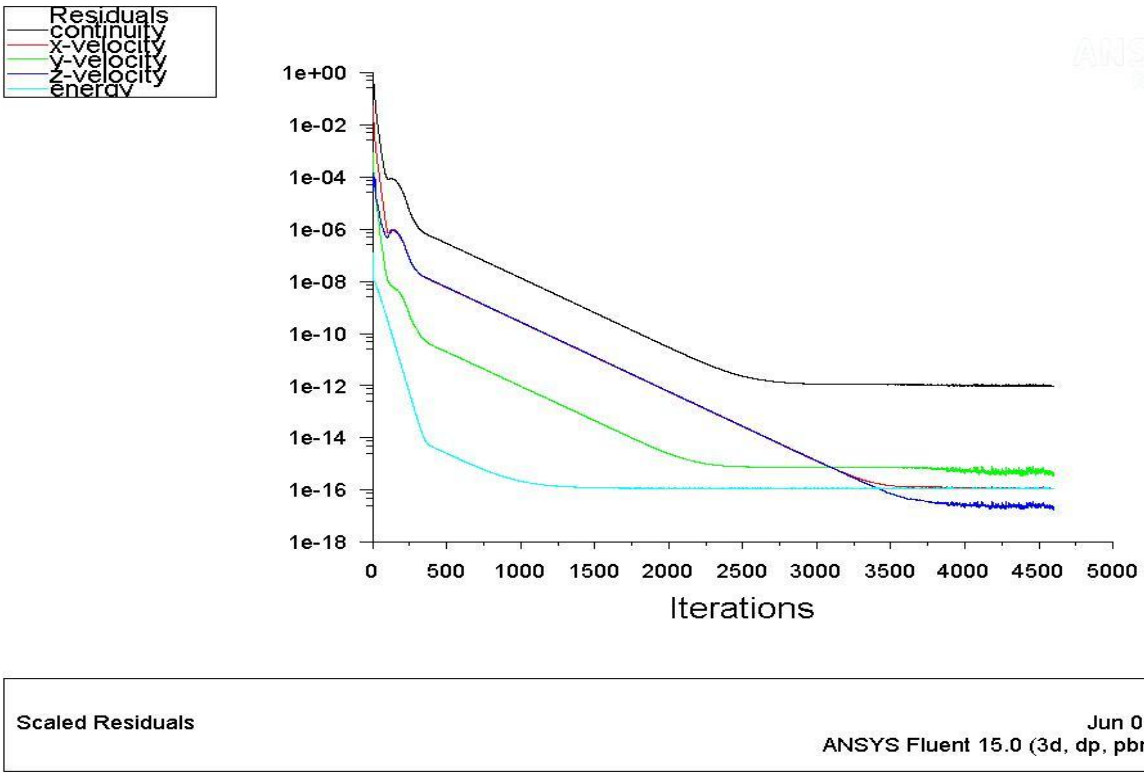
Residuals
continuity
x-velocity
y-velocity
z-velocity
energy
1e+00
1e-02
1e-04
1e-06
1e-08
1e-10
1e-12
1e-14
1e-16
1e-18
0
500
1000
1500
2000
2500
3000
3500
4000
4500
5000
Iterations
Scaled Residuals
Jun 07, 2015
ANSYS Fluent 15.0 (3d, dp, pbns, lam)

Case-4

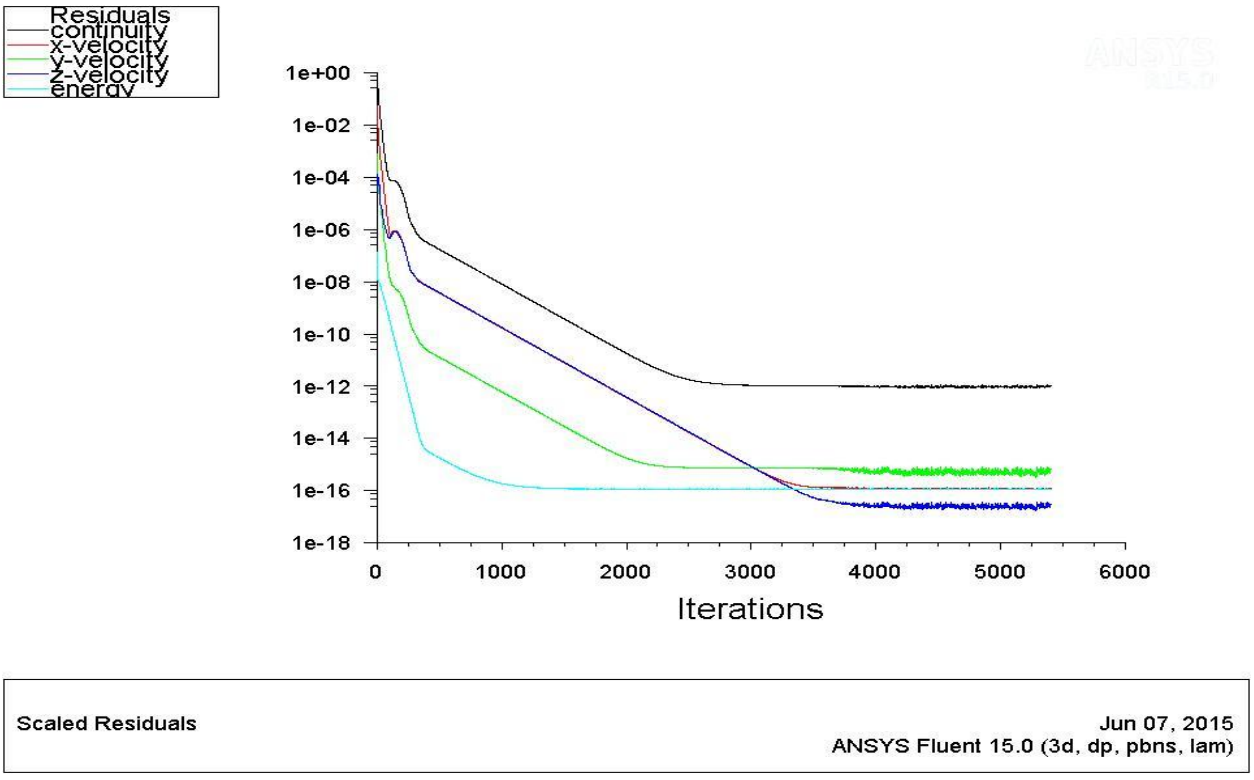
Residuals
continuity
x-velocity
y-velocity
z-velocity
energy
1e+00
1e-02
1e-04
1e-06
1e-08
1e-10
1e-12
1e-14
1e-16
1e-18
0
1000
2000
3000
4000
5000
6000
Iterations
Scaled Residuals
Jun 07, 2015
ANSYS Fluent 15.0 (3d, dp, pbns, lam)

Case-5

ANNEX-II

CELL TEMPERATURE

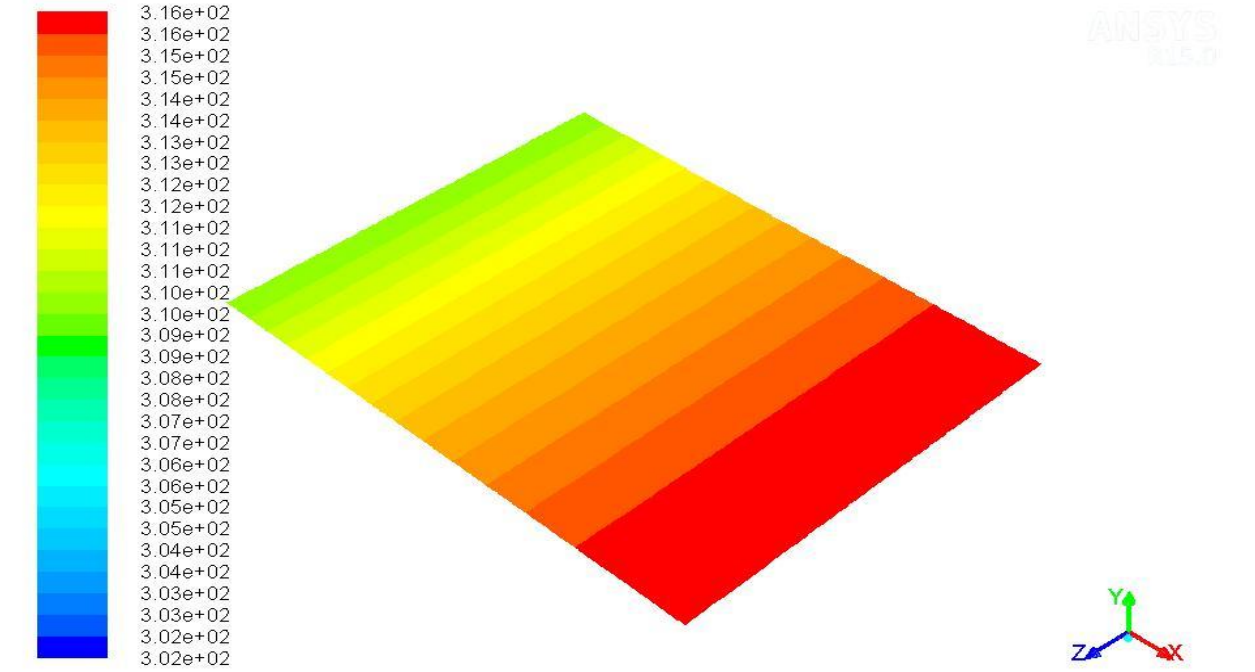

Case-1

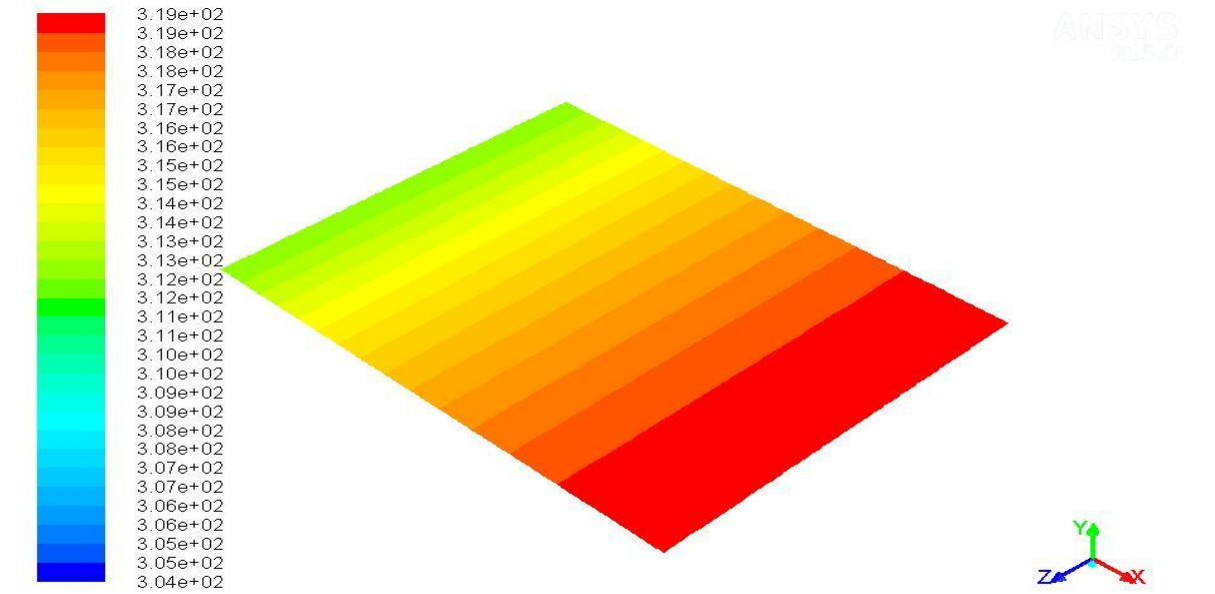
3.19e+02
3.19e+02
3.18e+02
3.18e+02
3.17e+02
3.17e+02
3.16e+02
3.16e+02
3.15e+02
3.15e+02
3.14e+02
3.14e+02
3.13e+02
3.13e+02
3.12e+02
3.12e+02
3.11e+02
3.11e+02
3.10e+02
3.10e+02
3.09e+02
3.09e+02
3.08e+02
3.08e+02
3.07e+02
3.07e+02
3.06e+02
3.06e+02
3.05e+02
3.05e+02
3.04e+02
Y
Z
X
Contours of Static Temperature (k)
Aug 03, 2015
ANSYS Fluent 15.0 (3d, dp, pbns, lam)

Case-2

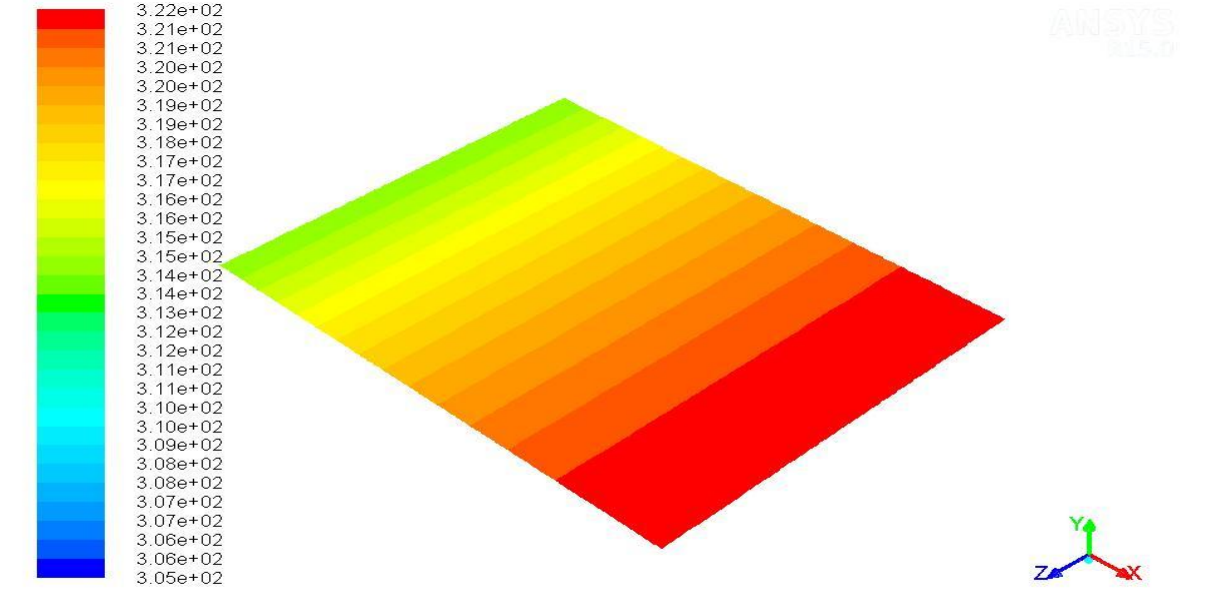
3.22e+02
3.21e+02
3.21e+02
3.20e+02
3.20e+02
3.19e+02
3.19e+02
3.18e+02
3.17e+02
3.17e+02
3.16e+02
3.16e+02
3.15e+02
3.15e+02
3.14e+02
3.14e+02
3.13e+02
3.12e+02
3.12e+02
3.11e+02
3.11e+02
3.10e+02
3.10e+02
3.09e+02
3.08e+02
3.08e+02
3.07e+02
3.07e+02
3.06e+02
3.06e+02
3.05e+02
Y
Z
X
Contours of Static Temperature (k)
Aug 03, 2015
ANSYS Fluent 15.0 (3d, dp, pbns, lam)

Case-3

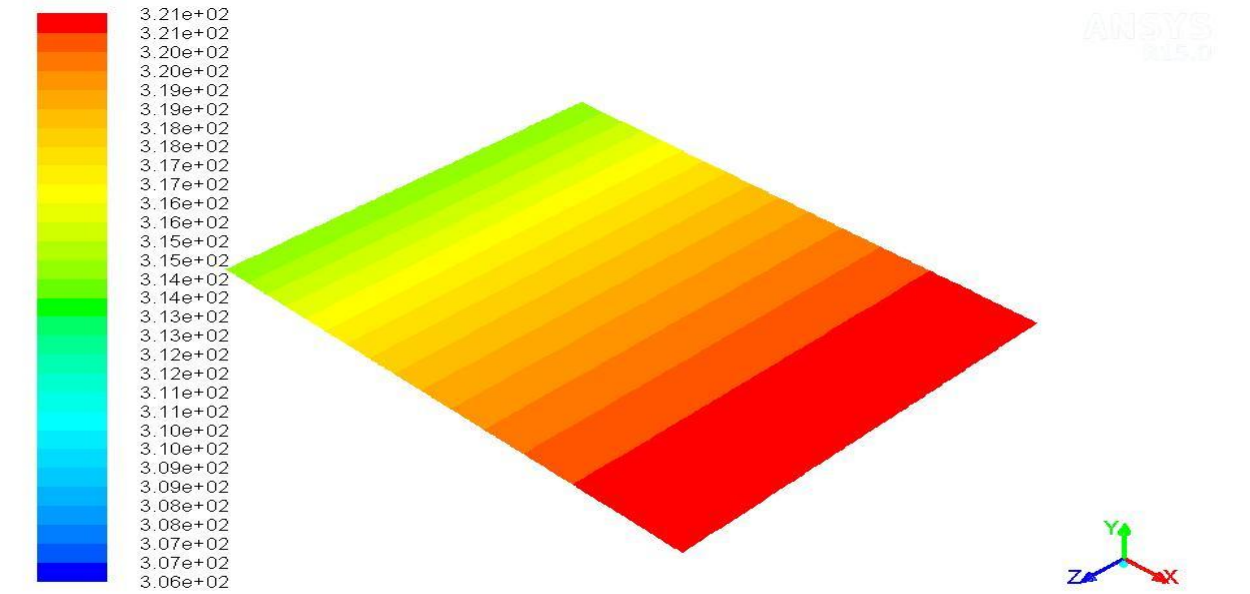
3.21e+02
3.21e+02
3.20e+02
3.20e+02
3.19e+02
3.19e+02
3.18e+02
3.18e+02
3.17e+02
3.17e+02
3.16e+02
3.16e+02
3.15e+02
3.15e+02
3.14e+02
3.14e+02
3.13e+02
3.13e+02
3.12e+02
3.12e+02
3.11e+02
3.11e+02
3.10e+02
3.10e+02
3.09e+02
3.09e+02
3.08e+02
3.08e+02
3.07e+02
3.07e+02
3.06e+02
Y
Z
X
Contours of Static Temperature (k)
Aug 03, 2015
ANSYS Fluent 15.0 (3d, dp, pbns, lam)

Case-4

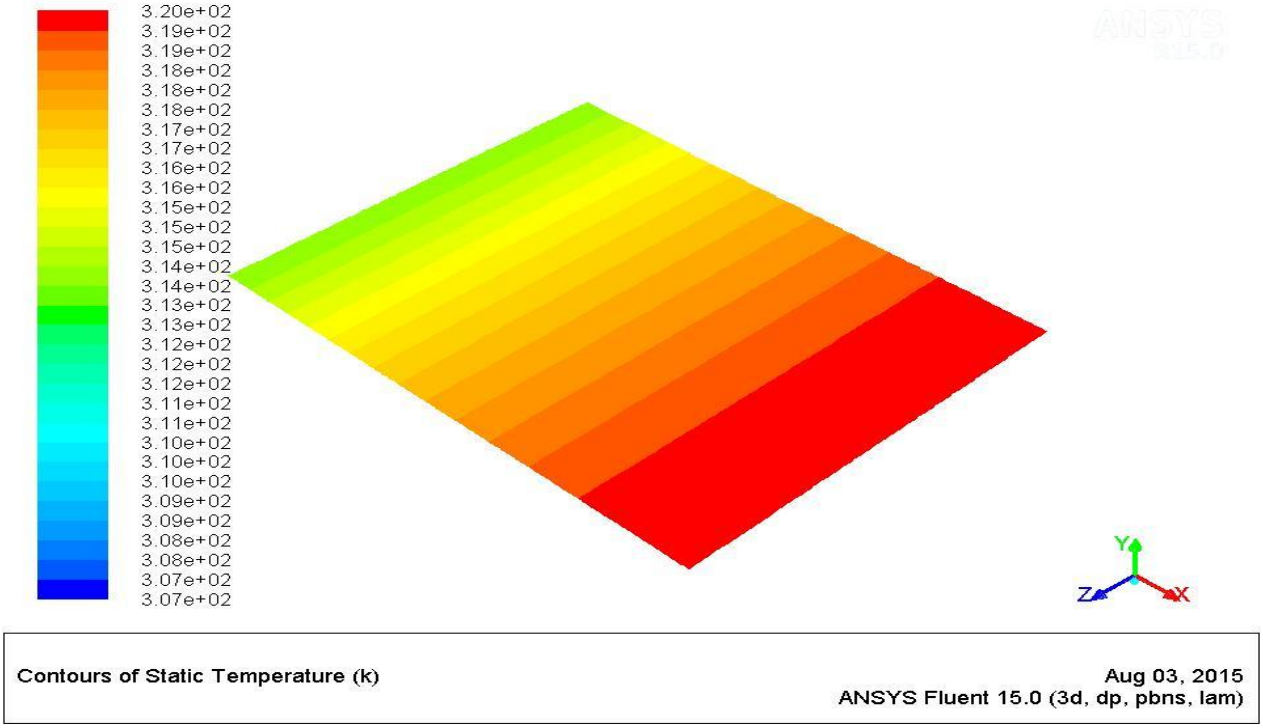
3.20e+02
3.19e+02
3.19e+02
3.18e+02
3.18e+02
3.18e+02
3.17e+02
3.17e+02
3.16e+02
3.16e+02
3.15e+02
3.15e+02
3.15e+02
3.14e+02
3.14e+02
3.13e+02
3.13e+02
3.12e+02
3.12e+02
3.12e+02
3.11e+02
3.11e+02
3.10e+02
3.10e+02
3.10e+02
3.09e+02
3.09e+02
3.08e+02
3.08e+02
3.07e+02
3.07e+02
Y
Z
X
Contours of Static Temperature (k)
Aug 03, 2015
ANSYS Fluent 15.0 (3d, dp, pbns, lam)

Case-5

ANNEX-III

Cell Temperature, Power & Efficiency Data

Day Time	Ambient Temp:	Solar Irradiance Heat Flux	Cell Temp: (Normal)	Cell Temp: (CFD Air Cooled)	Temp: Diff:	Power (Normal)	Power (CFD Air cooled)	Power Diff:	Efficiency (Normal)	Efficiency (CFD Air cooled)	Efficiency Diff:
	A	B	C	D	E= C- D	F	G	H= G-F	I	J	K= J-I
Hrs	˚C	W/m^2	˚C	˚C	˚C	W	W	W	%	%	%
10:00 am	29	625	48	40.3	7.7	4.37	4.47	0.11	5.47	5.60	0.13
11:00 am	31	700	53	40.8	12.2	5.39	5.60	0.21	6.76	7.02	0.26
12:00 pm	32	750	54	43.8	10.2	6.17	6.37	0.20	7.73	7.98	0.25
13:00 pm	33	700	55	46.2	8.8	5.36	5.51	0.15	6.71	6.90	0.19
14:00 pm	34	600	54	45.7	8.3	3.95	4.05	0.11	4.95	5.08	0.13

Normal: Conventional Photovoltaic Module

CFD Air Cooled: Modified Photovoltaic Module